Systems Biology Approaches to Metabolic Health

Shankar Subramaniam
University of California San Diego

NASEM- Precision Medicine: Promoting Knowledge Exchange and Collaboration between Kuwait and the United States – Workshop Series. Oct 15, 2025

Why metabolomics?

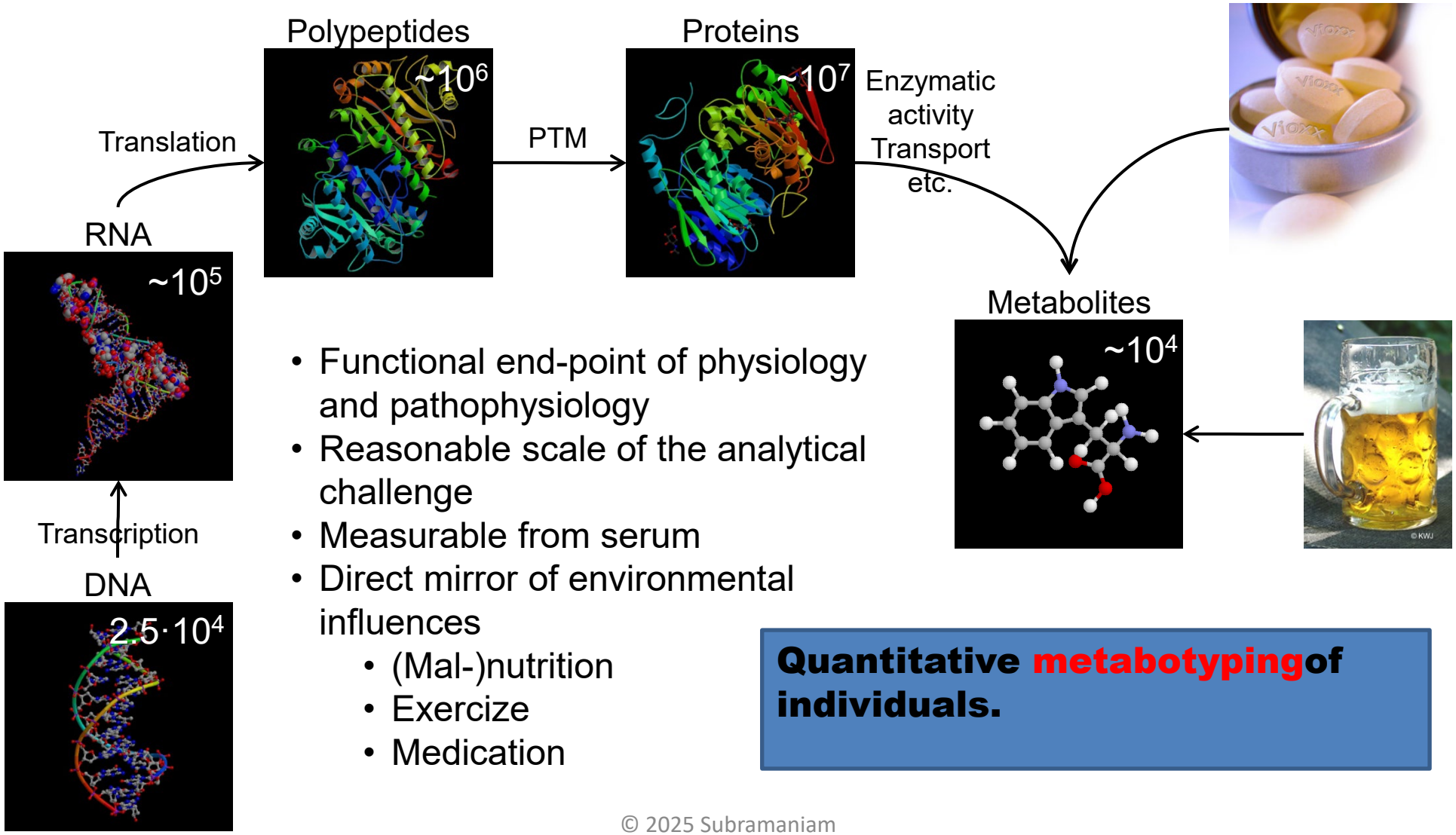

- Functional end-point of physiology and pathophysiology
- Reasonable scale of the analytical challenge
- Measurable from serum
- Direct mirror of environmental influences
  - (Mal-)nutrition
  - Exercize
  - Medication

Quantitative metabotypingof individuals.

Metabolomics Workbench and LIPIDMAPS – A 20-year journey

Acknowledgments

LIPIDMAPS – NIH NIGMS GLUE GRANT
WELLCOME TRUST GRANT
METABOLOMICS WORKBENCH – NIH CF
CFDE Data Resource Center – NIH CFDE GRANT

Eoin Fahy (MW and LIPIDMAPS)
Mano Maurya (MW)
Srini Ramachandran (MW)
Andrew Caldwell (MW)
Kevin Coakley (MW)
Christine Kirkpatrick (MW)
Neela Srinivasan (MW)
Shashidhar Rao (MW)
Shakti Gupta (MW)
Manish Sud (MW and LIPIDMAPS)
Kenan Azam (MW)
Lina Aboulmona (MW)
Kim Ngo (MW)
Dawn Cotter (LIPIDMAPS)
Sonal Chowdhary (MW)
Robert Byrnes (MW and LIPIDMAPS)
Andrea Meyer (LIPIDMAPS)
Bryan Saunders (MW and LIPIDMAPS)

LIPIDMAPS Glue Grant Teams
LIPIDMAPS UK Teams
Metabolomics Common Fund Project Teams

METABOLOMICS WORKBENCH AND INFRASTRUCTURE: A GATEWAY TO MULTIOMICS INTEGRATION AND DISEASE BIOLOGY

Shankar Subramaniam, UC San Diego

Metabolomics Workbench website

https://www.metabolomicsworkbench.org

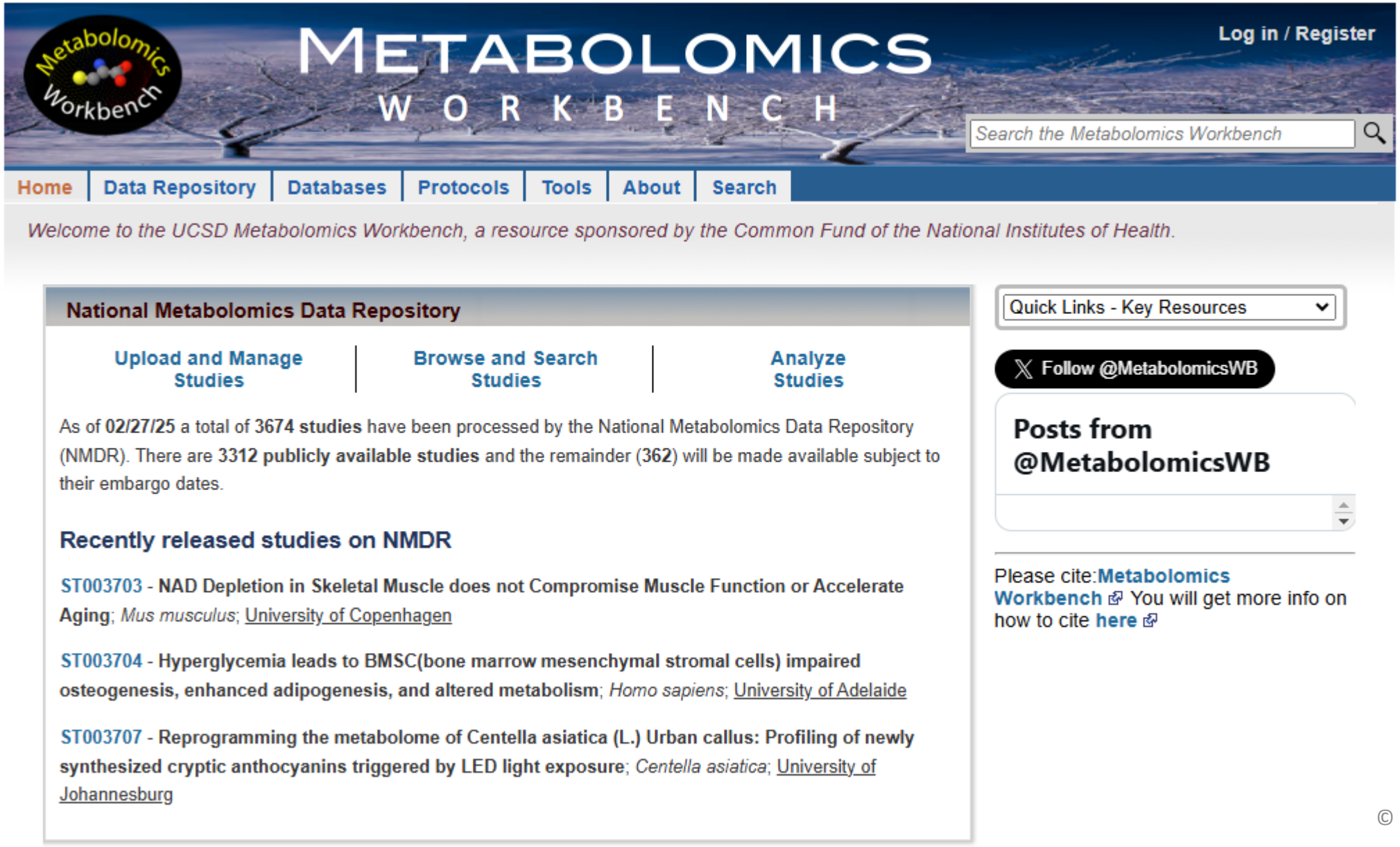

Metabolomics Workbench

https://www.metabolomicsworkbench.org

NMDR Summary table as of 10/13/25		
Category	**All studies**	**Public studies**
Number of studies in NMDR	4197	3780
Number of human studies in NMDR	1726	1547
Number of samples	465783	396074
Number of named metabolites submitted to NMDR	975274	869086
Number of named metabolites mapped to RefMet	810058	731092
Number of data points for named metabolites	75416830	67823501
Number of unknown MS features (m/z, rt values) in NMDR	12249351	11058183
Number of Sample sources in NMDR studies	310	284
Number of Species in NMDR studies	404	383
Number of Disease associations in NMDR studies	244	232
Number of Countries represented	51	49
Number of Institutes represented	678	642
Number of studies with LC-MS data	3276	2909
Number of studies with GC-MS data	555	528
Number of studies with NMR data	299	281
Number of metabolite species names in RefMet	190562	
Number of metabolite structures in the Metabolite structure database	175415	
Number of raw files (approximate)	500000	

Integration of Metabolomics with other Omics

A study of fatty liver disease

Gorden DL, Myers DS, Ivanova PT, Fahy E, Maurya MR, Gupta S, Min J, Spann NJ, McDonald JG, Kelly SL, Duan J, Sullards MC, Leiker TJ, Barkley RM, Quehenberger O, Armando AM, Milne SB, Mathews TP, Armstrong MD, Li C, Melvin WV, Clements RH, Washington MK, Mendonsa AM, Witztum JL, Guan Z, Glass CK, Murphy RC, Dennis EA, Merrill AH Jr, Russell DW, Subramaniam S, Brown HA. Biomarkers of NAFLD progression: a lipidomics approach to an epidemic. J Lipid Res. 2015 Mar;56(3):722-36.

Zarrinpar A, Gupta S, Maurya MR, Subramaniam S, Loomba R. Serum microRNAs explain discordance of non-alcoholic fatty liver disease in monozygotic and dizygotic twins: a prospective study.Gut. 2015 May 22. pii: gutjnl-2015-309456.

Non Alcoholic Fatty Liver Disease (NAFLD)

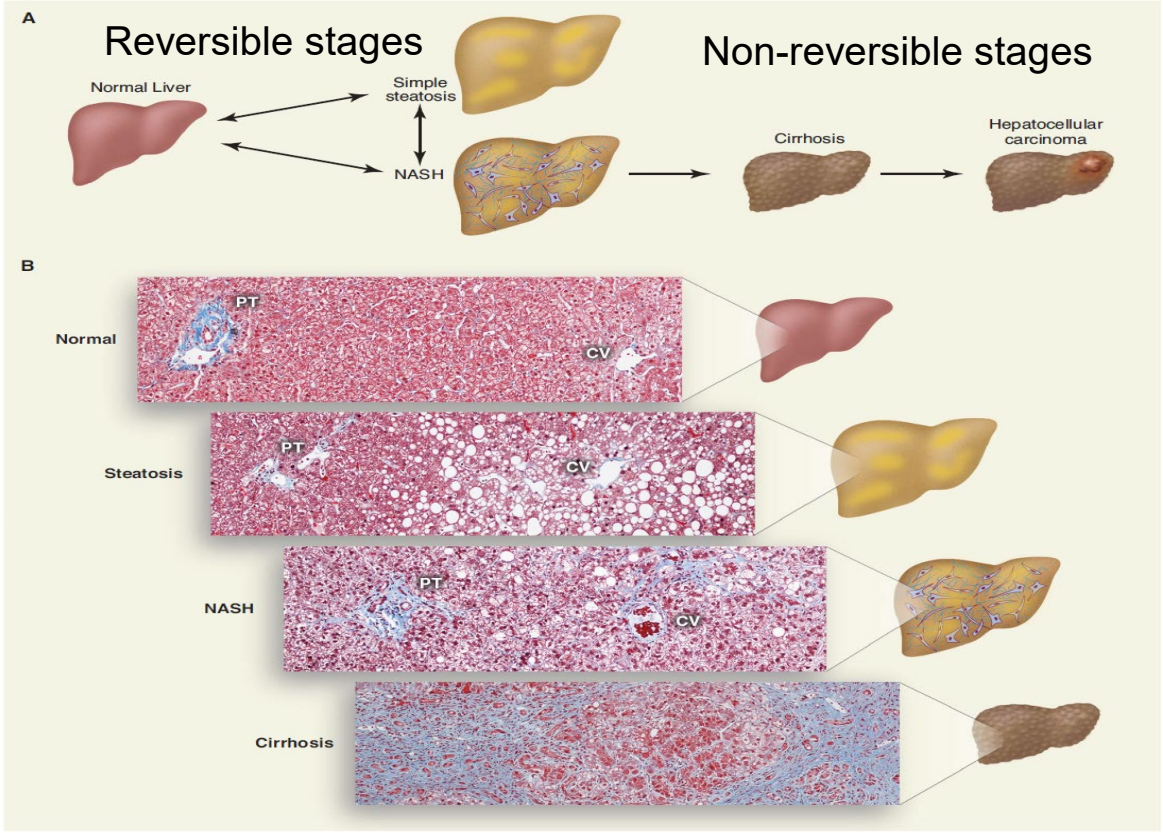

Cohen et al. 2011, Science

Liver Study

	Normal (n = 31)	Steatosis (n = 17)	NASH (n = 20)	Cirrhosis (n = 20)	*P* (Over Four States)	Post hoc (Steatosis vs. NASH)	Post hoc (NASH vs. Cirrhosis)
Gender (% female)	80.6	70.6	55.0	25.0	8.0E-04	NS	NS
Ethnicity (% white)	67.7	100.0	80.0	90.0	NS	NS	NS
BMI (kg/m^2)	40.1 ± 1.7	46.4 ± 2.7	47.5 ± 2.9	31.8 ± 1.5	2.3E-05	NS	[a]
Age (years)	48.1 ± 2.6	48.4 ± 2.8	47.6 ± 2.7	58.1 ± 2.0	1.8E-02	NS	[b]
Glucose (mg/dl)	110.3 ± 4.7	118.2 ± 10.9	128.9 ± 8.7	122.5 ± 10.6	NS	NS	NS
AST (U/l)	30.3 ± 4.6	26.4 ± 3.8	26.8 ± 2.2	62.7 ± 11.1	4.5E-03	NS	[c]
ALT (U/l)	28.5 ± 4.5	24.5 ± 2.9	31.0 ± 4.0	36.4 ± 4.6	NS	NS	NS
AlkP (U/l)	83.7 ± 5.8	74.1 ± 4.4	76.8 ± 5.1	116.6 ± 14.9	2.9E-02	NS	[c]
Total bilirubin (mg/dl)	0.45 ± 0.05	0.53 ± 0.04	0.43 ± 0.06	6.3 ± 2.0	3.8E-03	NS	[c]

Data are expressed as mean ± SEM. Indicators, such as aspartate aminotransferase (AST), alanine aminotransferase (ALT), alkaline phosphatase (AlkP), and total bilirubin failed to show a strong difference between steatosis and NASH. Statistical testing across all four histological types was by chi-squared test for gender and ethnicity and ANOVA for all others. Post hoc testing of steatosis versus NASH and NASH versus cirrhosis for clinical data was conducted by Welch test (to control for unequal variances) for continuous variables and by chi-squared test for gender and ethnicity. Bonferroni corrected significance of the post hoc tests is indicated.

[a] $P < 0.001$.

[b] $P < 0.01$.

[c] $P < 0.05$.

Common metabolites between liver and plasma. Major lipid classes, DAGs, TAGs, CEs, and GPLs are almost all polyunsaturated while sphingo-lipids are primarily longer chain species

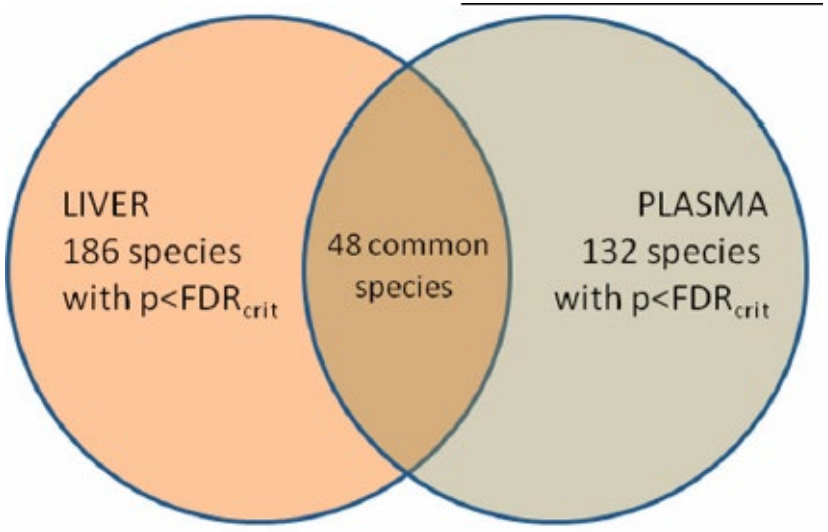

1,2-DAG(34:2)	Lanosterol	C18 Cer
1,2-DAG(36:2)	14-desmethyl-14-dehydrolanosterol	C20 Cer
1,2-DAG(36:3)	27-hydroxycholesterol	C22 Cer
TAG(50:2)	3-oxo,7α-hydroxycholesterol	C24 Cer
TAG(52:1)	7α-hydroxycholesterol	C18DH 1-deoxyCer
TAG(52:3)	12-HETE	C20DH 1-deoxyCer
TAG(52:4)	15-HETrE	C22DH 1-deoxyCer
TAG(52:5)	LTE4	C24DH 1-deoxyCer
TAG(54:3)	LPC(18:0)	C24:1DH Cer
TAG(54:4)	PC(36:4)	C24 GlcCer
TAG(54:5)	PC(38:4)	C24 HexCer
TAG(56:6)	PE(36:3)	C22 Sphingomyelin
CE(18:2)	PE(38:4p)	Sphingosine
CE(20:3)	PE(38:6)	Sphingosine-P
CE(20:4)	PE(40:6)	F16BP
CE(22:6)	PI(36:3)	Dolichol-20

Fold changes (log2) for species with FDR-adjusted significant P-values A. Liver, B. Plasma

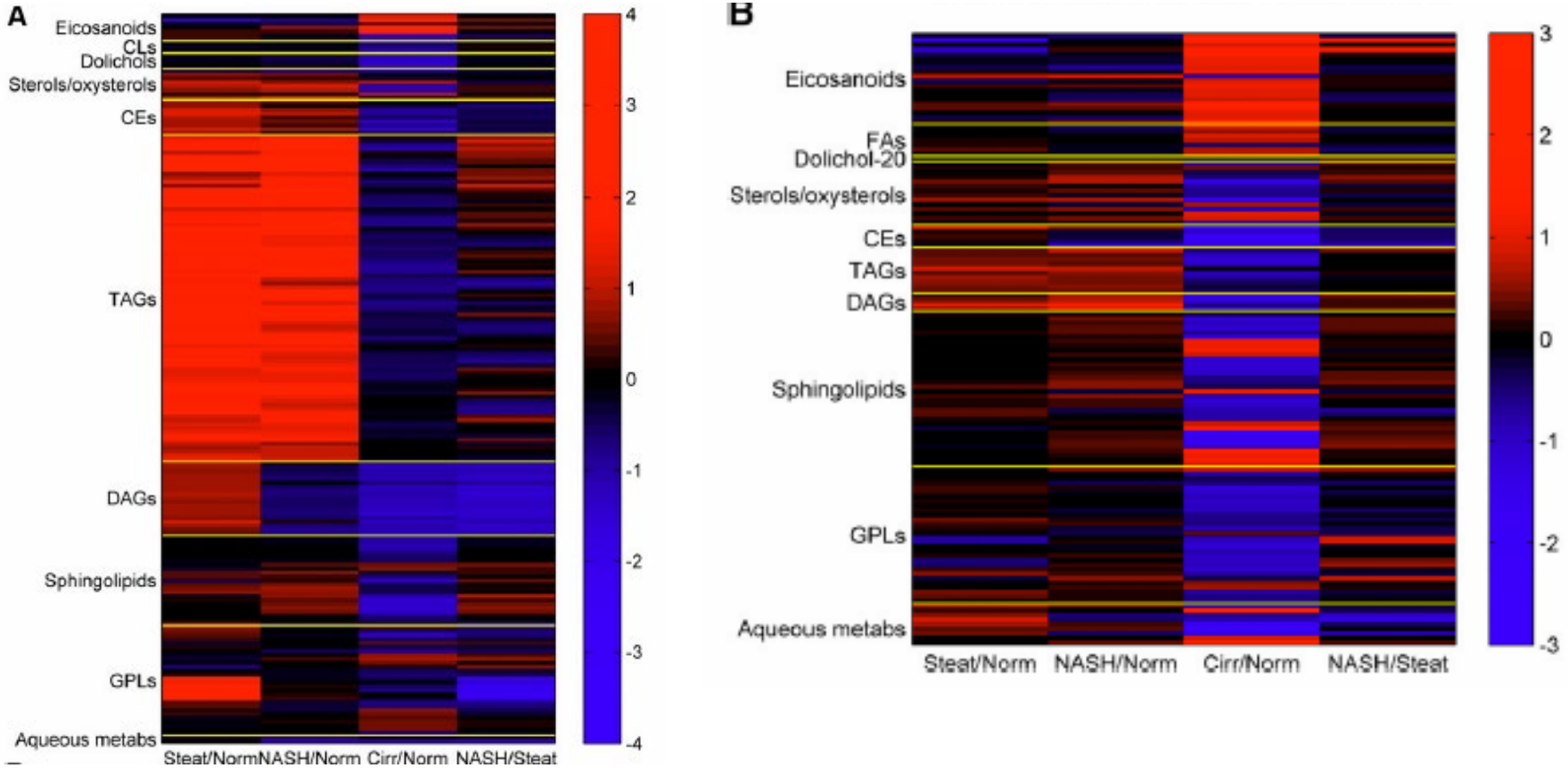

LDA on plasma (A) liver species (B) with top 80 ANOVA scores classified samples by disease status. Blue: steatosis, black: normal; orange: steatohepatitis; red: cirrhosis

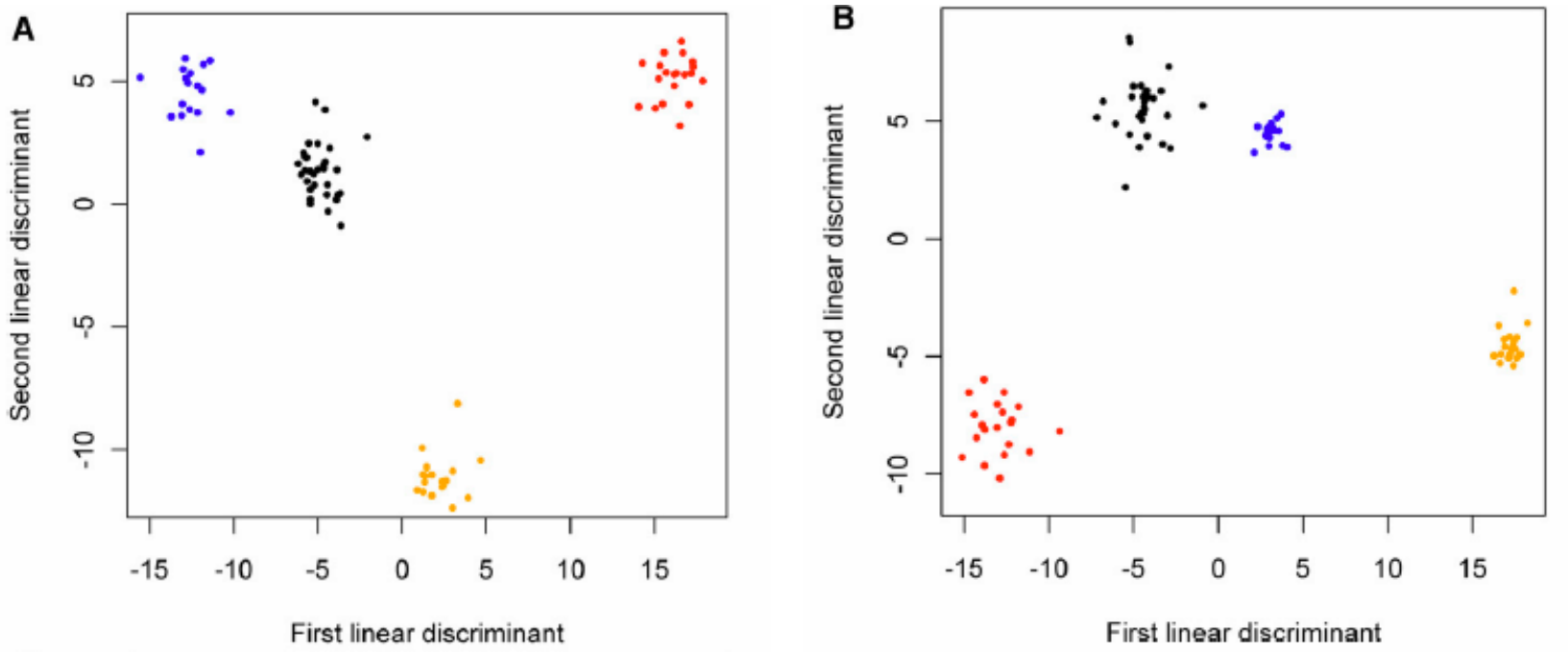

A

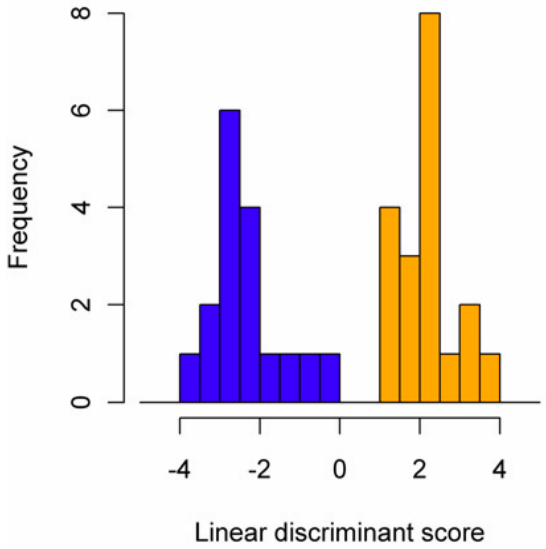

B

Species	Fold (NASH/steatosis)
PC(32:0)	1.39
PC(36:0e)	0.70
PC(36:1e)	0.73
PC(36:2e)	0.67
PE(36:3)	0.80
PI(32:1)	1.69
LPI(18:0)	0.42
LPI(20:4)	0.55
CE(22:6)	0.52
Dolichol-20	1.20
24,25-epoxycholesterol	1.46
FA(20:2)	0.75
C14DH Cer	0.77
C24:1DH 1-deoxyCer	1.60
C26DH 1-deoxyCer	1.92
C26:1DH HexCer	0.51
Sphingosine	0.62
F16BP	0.48
PGA	0.39
AMP	0.57

A: Histogram of LDA results from the 20 plasma metabolites having the most statistically significant differences between NASH and steatotic samples as demonstrated by *P* values. When these species are used for classifi cation, the two disease states are clearly distinguished. Blue, steatosis; orange, steatohepatitis. B: The list of 20 species used in (A) shows that a diverse spectrum of lipids and aqueous metabolites make up the signature distinguishing steatosis and NASH.

Liver transcripts for all collagen genes showing upregulation with progression of disease

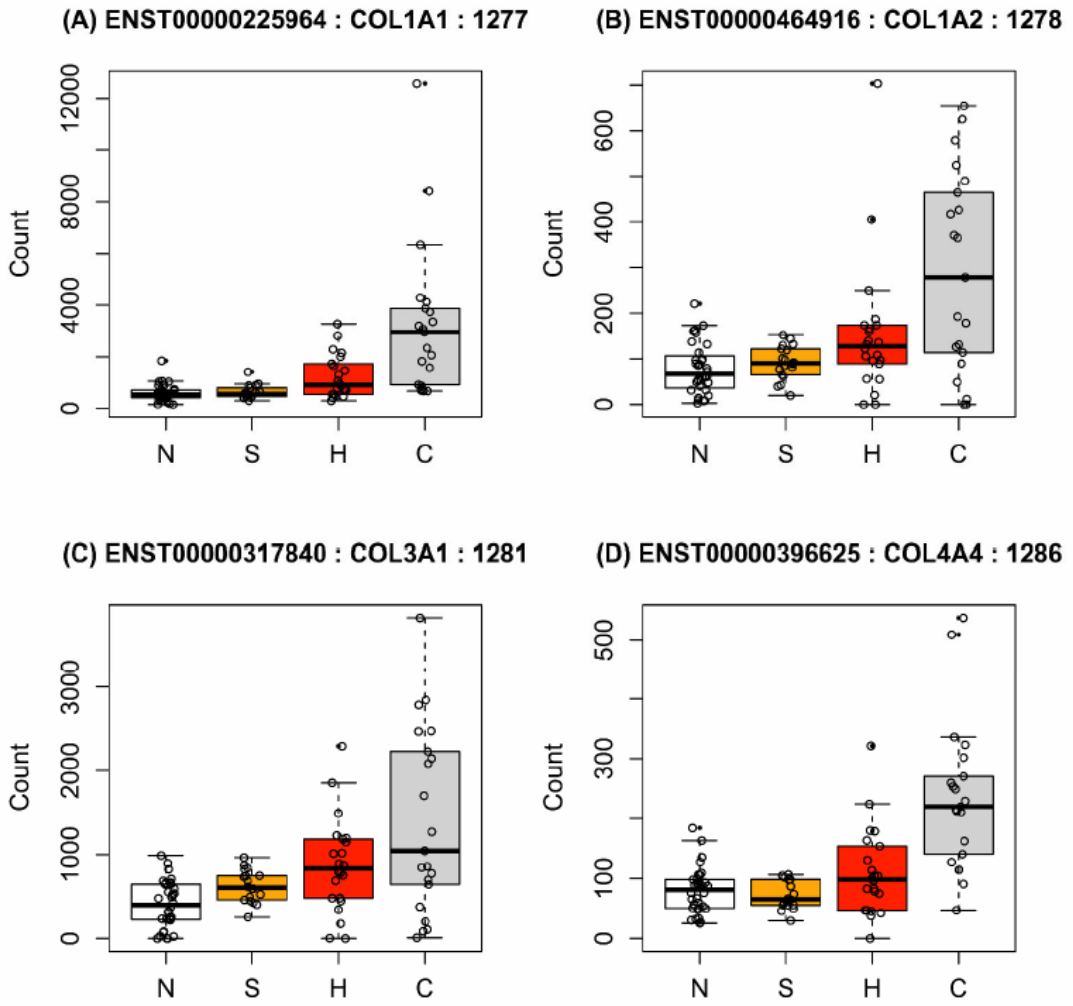

Liver transcripts for IL1b, TGFb1, CCL2, CXCL1, MMP9 show upregulation with disease progression. MMP14 shows upregulation between cirrhosis and other disease stages

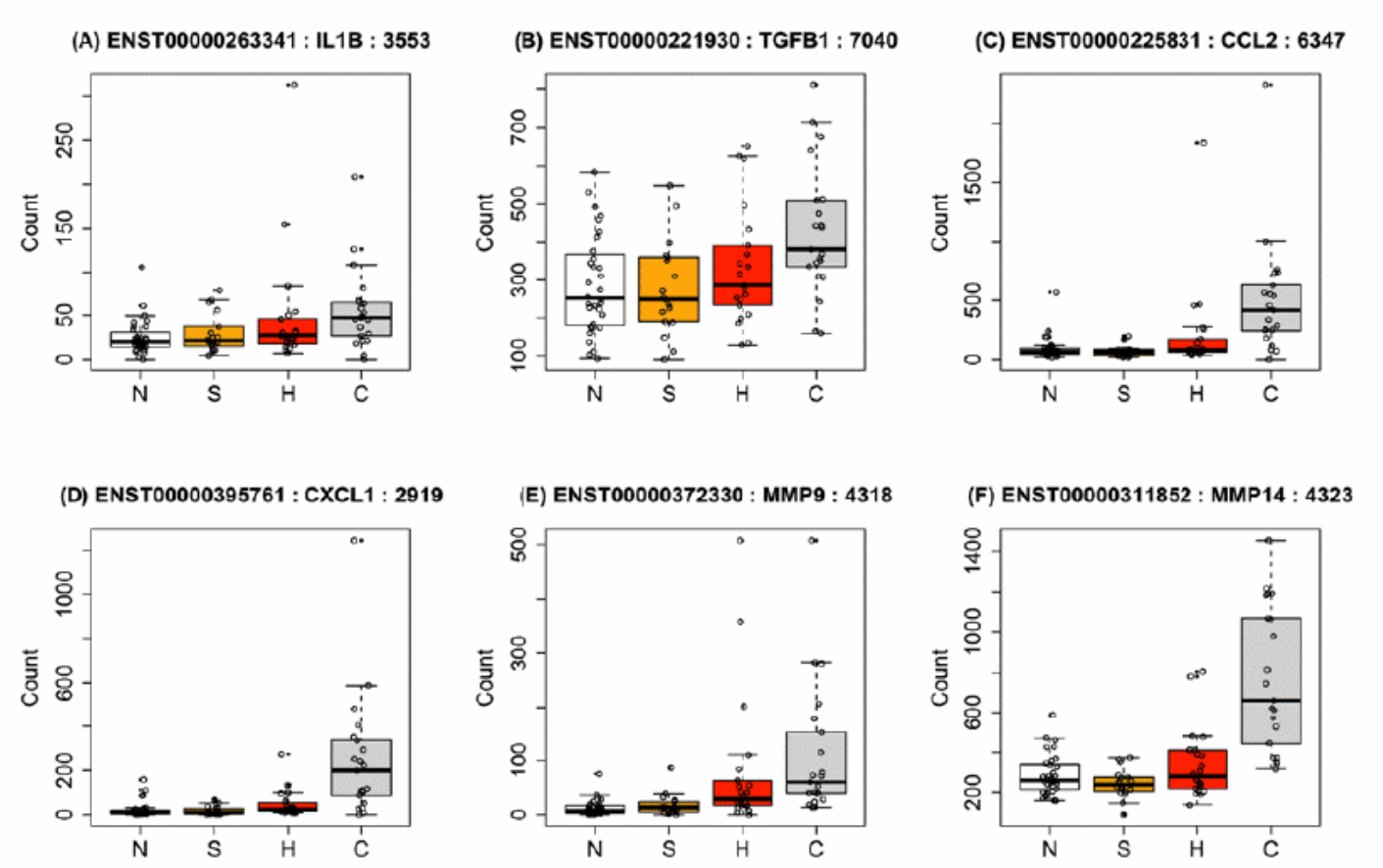

Table S3. Single nucleotide polymorphisms with P<0.001 for steatosis vs. NASH, assessed using PLINK.

SNP	Gene	P-value	Odds ratio	Alleles [WT/ mutation]	Mutation information
rs3747636	PIK3C2B	1.26E-04	0.09	[A/G]	Synonymous_N1198N
rs7257872	ZNF584	2.51E-04	20.67	[A/G]	Missense_T301A
rs2010834	KATNAL2	3.37E-04	6.23	[A/C]	Silent,Missense_C254F
exm110947	PEAR1	4.90E-04	18.60	[A/G]	Missense_R885H
rs882610	ZNF446	4.90E-04	18.60	[A/G]	Missense_R387H
rs17795400	EFHB	7.81E-04	0.12	[A/C]	Missense_G99V
exm529135	VARS2	9.35E-04	16.69	[A/G]	Missense_R777Q,Missense_R917Q,Missense_R947Q

Table S4 . Single nucleotide polymorphisms with P<0.0001 for normal vs. cirrhosis, assessed using PLINK.

SNP	Gene	P	Odds Ratio	Alleles	Mutation
rs738409	PNPLA3	1.77E-06	9.603	[C/G]	Missense_I148M
exm1032658	NUAK1	2.39E-05	11.8	[C/G]	Missense_P543R
exm8127	AJAP1	2.68E-05	0.143	[A/G]	Missense_G263R
rs185200	ARHGAP26	3.06E-05	0.136	[A/G]	Synonymous_R85R
rs9482	ATF6	3.27E-05	0.126	[A/G]	Synonymous_S632S
rs3761472	SAMM50	4.03E-05	7.636	[A/G]	Missense_D110G

Metabolomics, Transcriptomics, & Epigenomics in Atherosclerosis

"Atherosclerotic cardiovascular disease is the leading cause of mortality worldwide."

Barquera, S., et al., Arch Med Res, 2015. **46**(5): p. 328-38.

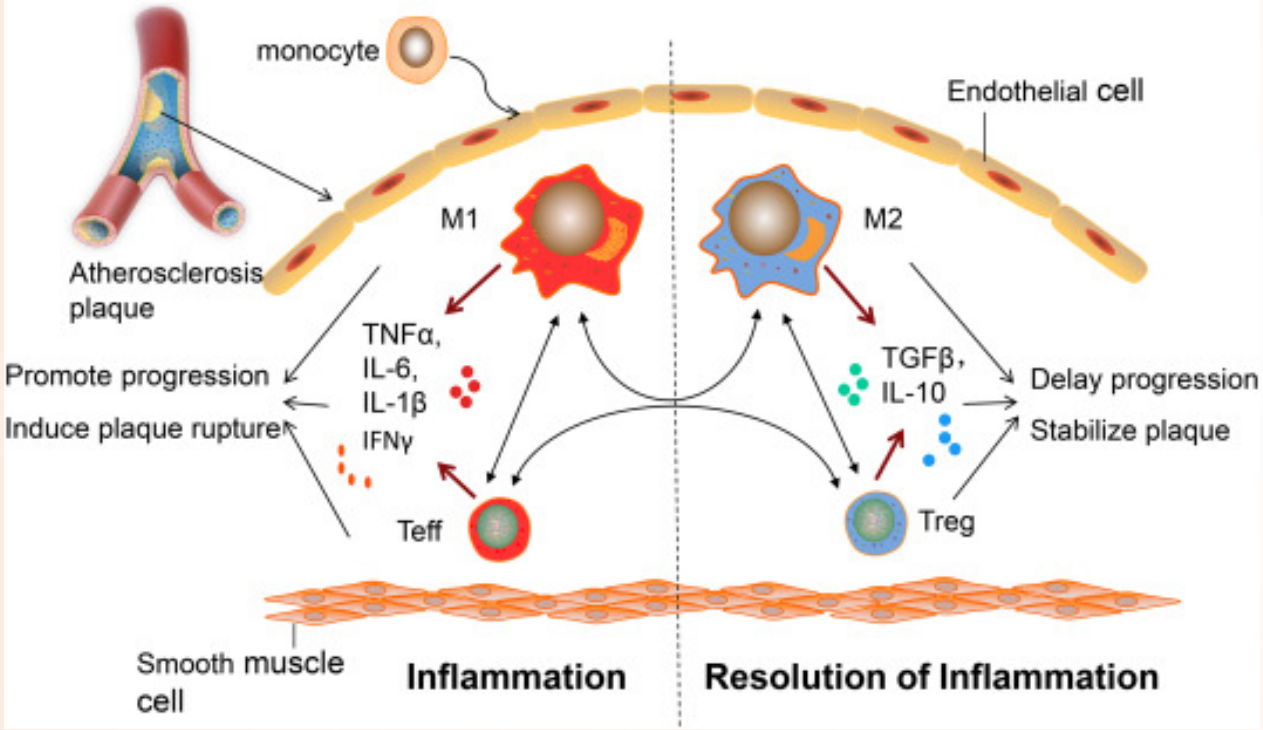

Song et al. Clinical Immunology Volume 202, May 2019, Pages 11-17

(Some) Causes of Plaque Formation

- Diet and other lifestyle choices
- Genetic predispositions
- Blood flow and shear stress

Metabolomics, Transcriptomics, & Epigenomics in Atherosclerosis

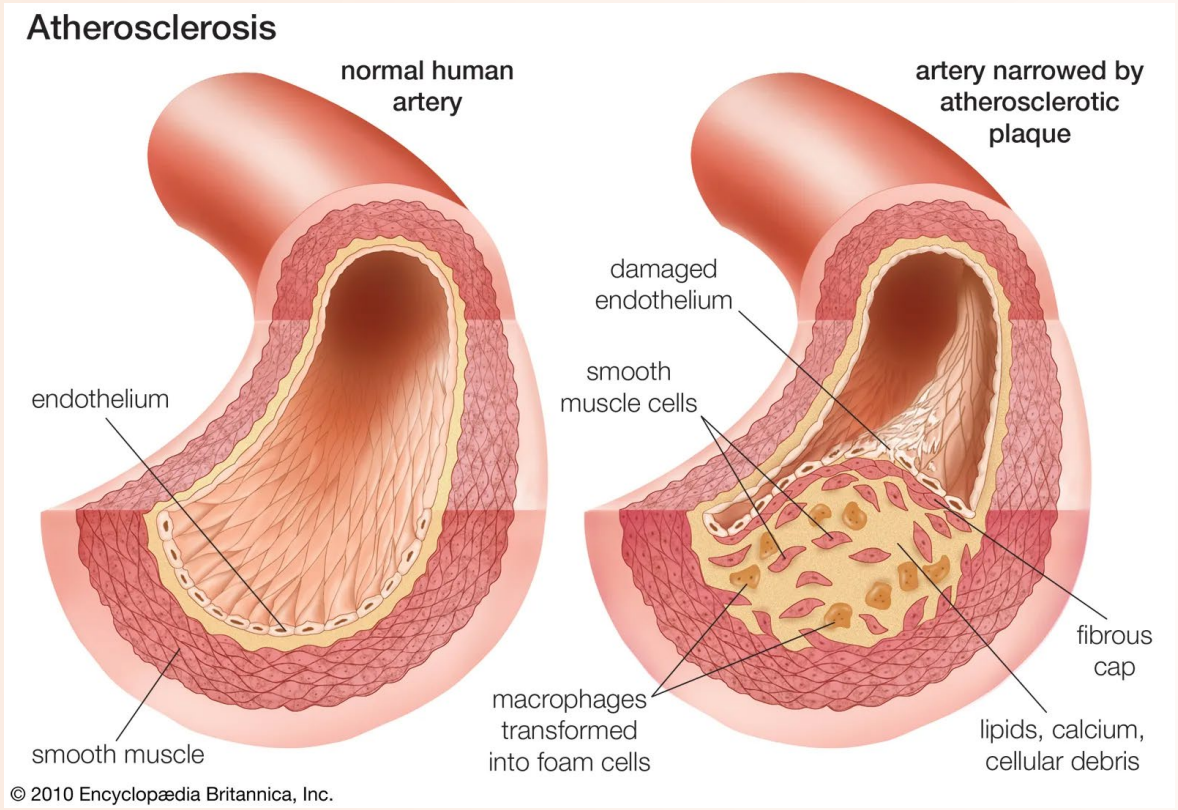

Britannica

"Atherosclerotic cardiovascular disease is the leading cause of mortality worldwide."

Barquera, S., et al., Arch Med Res, 2015. **46**(5): p. 328-38.

(Some) Causes of Plaque Formation

- Diet and other lifestyle choices
- Genetic predispositions
- Blood flow and shear stress

Studying ECs *in vitro*

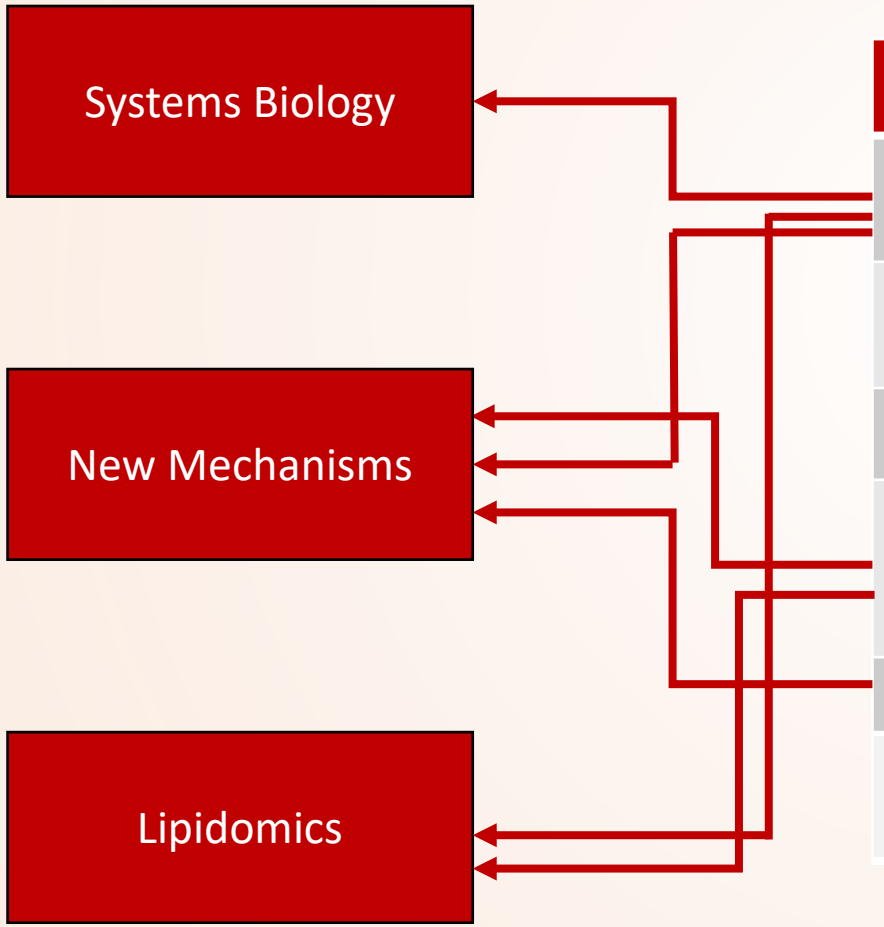

Data Type	Experiment Details	Conditions
RNA-seq	Time-series shear 10 time points	OS, PS, “low flow” (~ST)
RNA-seq	Overexpression	KLF2, SREBP2, AMPK, AMPK + SIRT1
RNA-seq	Shear, 16 hours	OS, PS
ChIP-seq	H3K27ac H3K27me3 H3K4me	OS, PS
4C	KLF2, NOS3 loci	OS, PS
Lipids/ genes	Endothelial Cells, Macrophages	Ch25h-/-, KLF4⇑

Systems Biology Summary

Integrating TF Information and Pathway Enrichment

Nassim Ajami

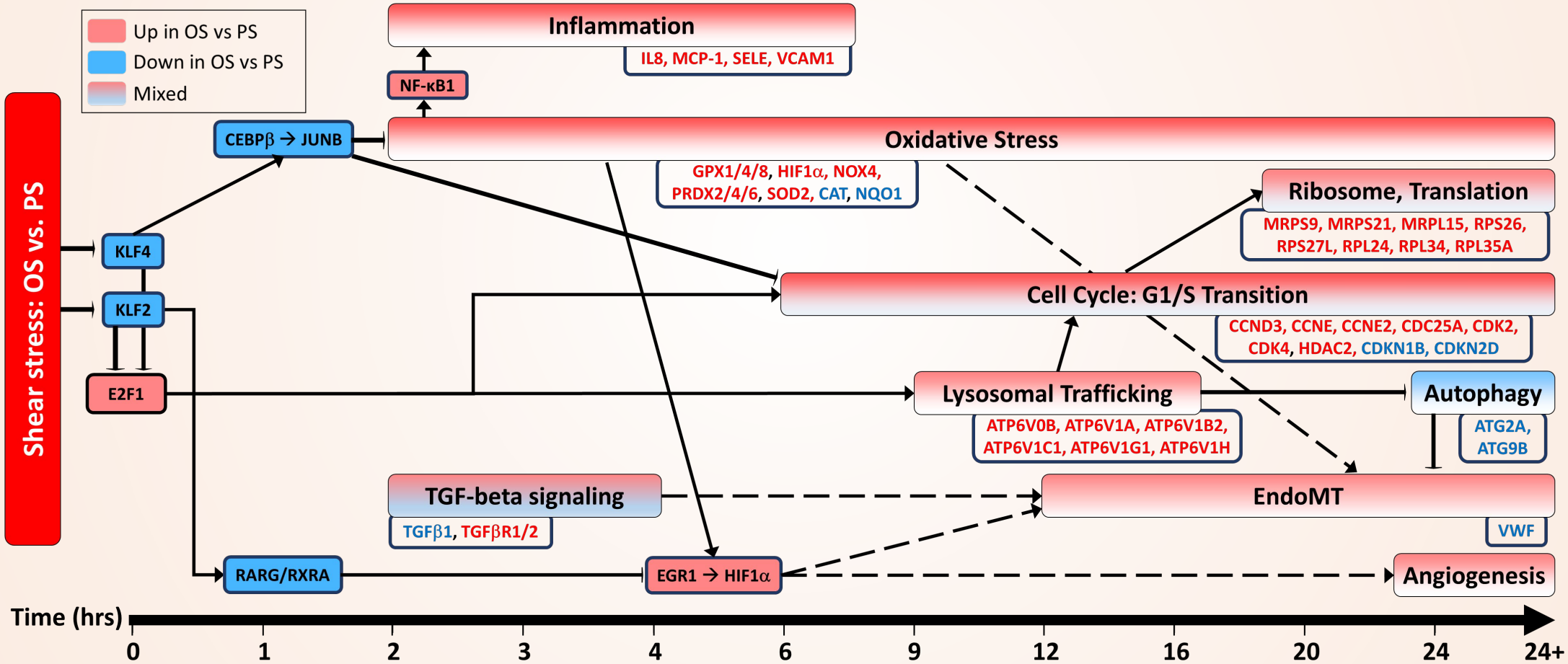

Ajami et al, PNAS 2017, PNAS 2021

New Mechanisms

Gene Analysis Through F.C. Comparisons Recovers Several Key EC genes

OS-Distinctive Genes	PS-Distinctive Genes
C9orf89, CCZ1, CD69, CXCR4, EIF2AK1, ENC1, ETV6, GLIPR1, GMFG, IDI1, KLHDC3, LIMS3, LYPLA2, MAGEF1, MEX3A, NFIL3, PAIP1, PCSK1, PDGFC, RNF145, SIRPA, STX6, TMEM155, TNFRSF21, WDR45L	ABCG2, ABLIM3, ACVRL1, ADAM15, ADAMTS4, ADARB1, AGXT2L2, ALS2CL, AMMECR1L, APOLD1, ARHGEF15, ARRDC2, ASAP2, ATG9B, C14orf34, C14orf49, C1orf21, C1QTNF6, C20orf160, CALML4, CARD14, CASKIN2, CCDC69, CLCF1, CRTAC1, CXCR7, DAG1, DENND4B, DGKA, DHH, DLL1, DNASE1L1, DOCK6, DUSP4, EFNB1, EHBP1L1, ENDOD1, ESAM, FAM124B, FAM65A, FGF2, FOXP1, GCH1, GCKR, GPD2, GPER, GRK5, HEG1, HR, HSPA12B, HSPA1A, HYAL1, HYAL2, IL3RA, INPP5K, ITGB4, ITGB5, ITPR3, ITSN2, JOSD1, KCNJ12, KIAA1161, KLF13, **KLF2, KLF4,** LPCAT4, LPHN2, MAP4K2, MBOAT1, MN1, MOB2, MYO1C, NAGA, NDRG4, NDST2, **NOS3**, NPEPPS, PLCD3, PLXND1, PMP22, PRUNE2, RAB11A, RBPMS, RECK, RNF213, RUSC1, S100A10, SEMA4B, SEPT8, SIGIRR, SLCO2A1, SORBS2, SPINK5, SPTBN1, SPTBN5, ST3GAL1, ST8SIA6, STARD8, STMN3, STOM, STXBP1, SULF1, TBC1D1, TBC1D2, TECPR1, TENC1, THBD, TINAGL1, TNFAIP1, TOB2, TRAK1, TRIM56, TSC22D3, UBE3B, VANGL1, VEGFA, XKR8, ZNF467

KLF2: Critical transcription factor for EC response to PS

Dekker RJ et al. Blood. 2002 Sep 1;100(5):1689-98.

KLF4: Similar to KLF2 in function, also important for PS-induced phenotype

Villarreal G et al. Biochem Biophys Res Commun. 2010 Jan 1;391(1):984-9.

NOS3: "Endothelial NOS" – produces nitric oxide and is crucial in regulating vascular tone

Förstermann U et al. Circulation. 2006 Apr 4;113(13):1708-14.

Lipidomics

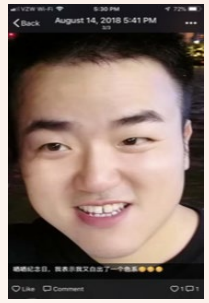


Li Zhao | Marcy Martin | Mano Maurya

KLF4 regulates cholesterol-25-hydroxylase and liver x receptor mitigating atherosclerosis susceptibility

Zhao, Martin, et al. Circulation, 2017

Vasoprotective stimuli increased the expression of Ch25h and LXR via KLF4. The KLF4-Ch25h/LXR homeostatic axis functions through suppressing inflammation, evidenced by the reduction of inflammasome activity in ECs and the promotion of M1 to M2 phenotypic transition in macrophages. The increased atherosclerosis in apolipoprotein $E^{-/-}$/$Ch25h^{-/-}$ mice further demonstrates the beneficial role of the KLF4-Ch25h/LXR axis in vascular function and disease.

KLF4 Mediates Cholesterol Homeostasis

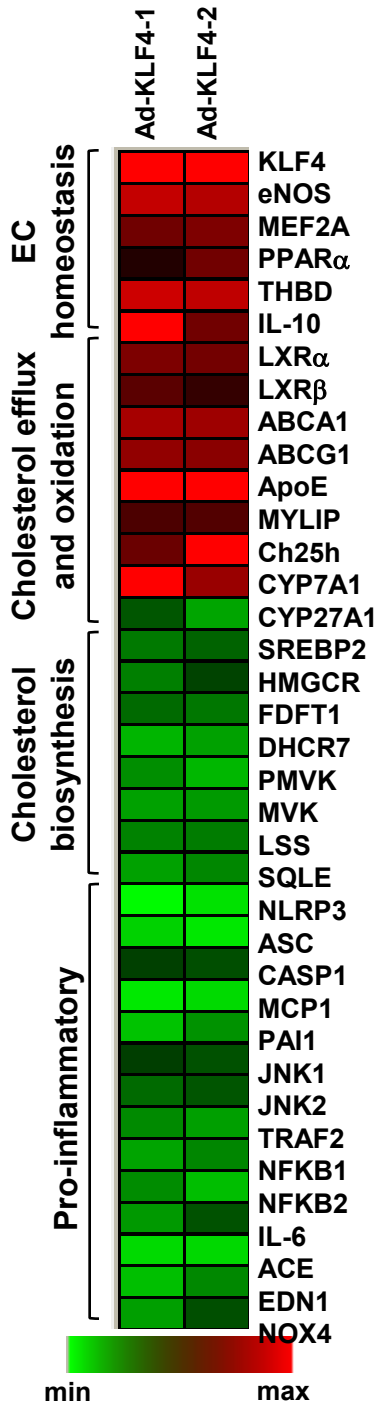

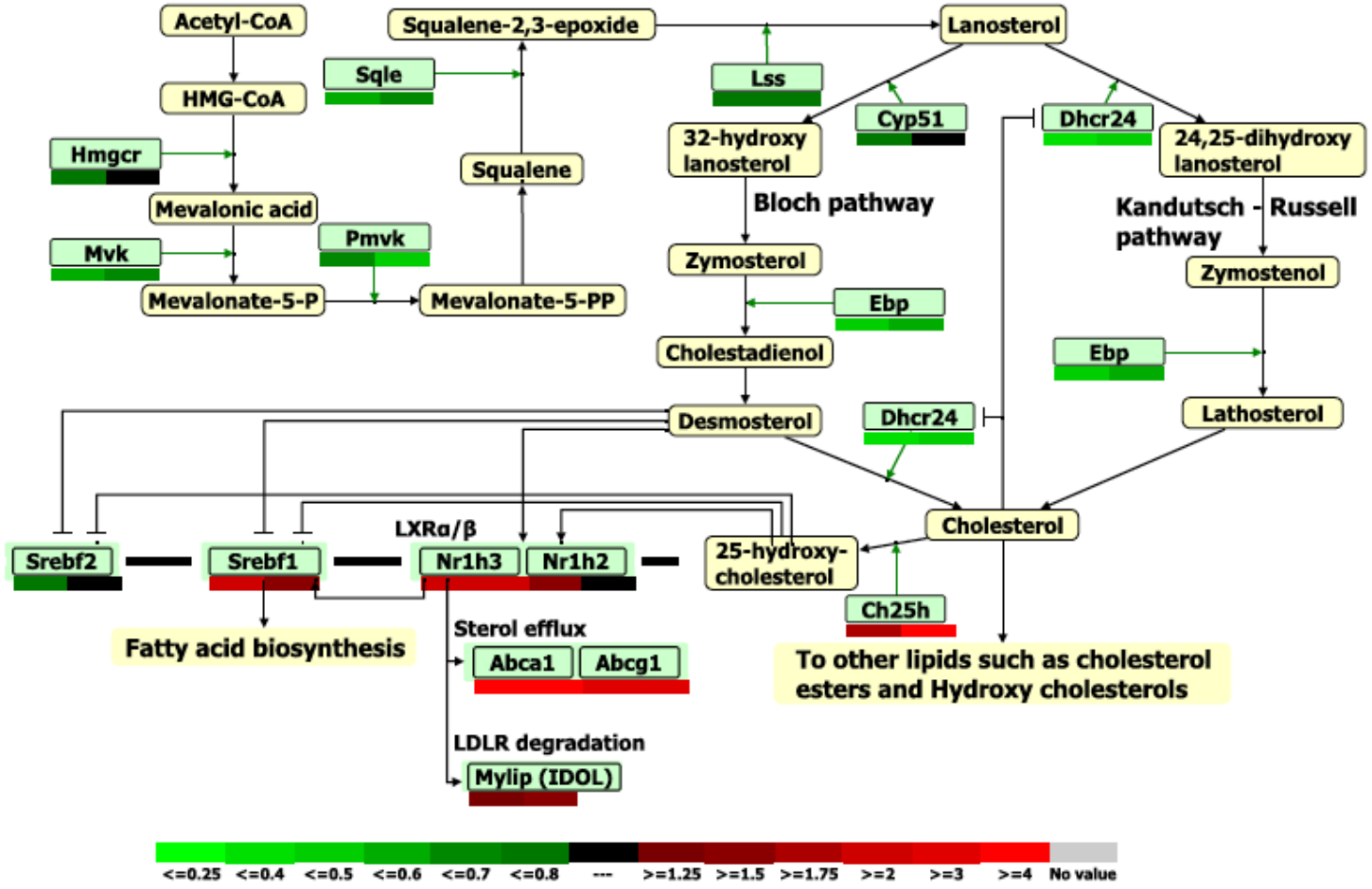

The Balance of Cholesterol Homeostasis

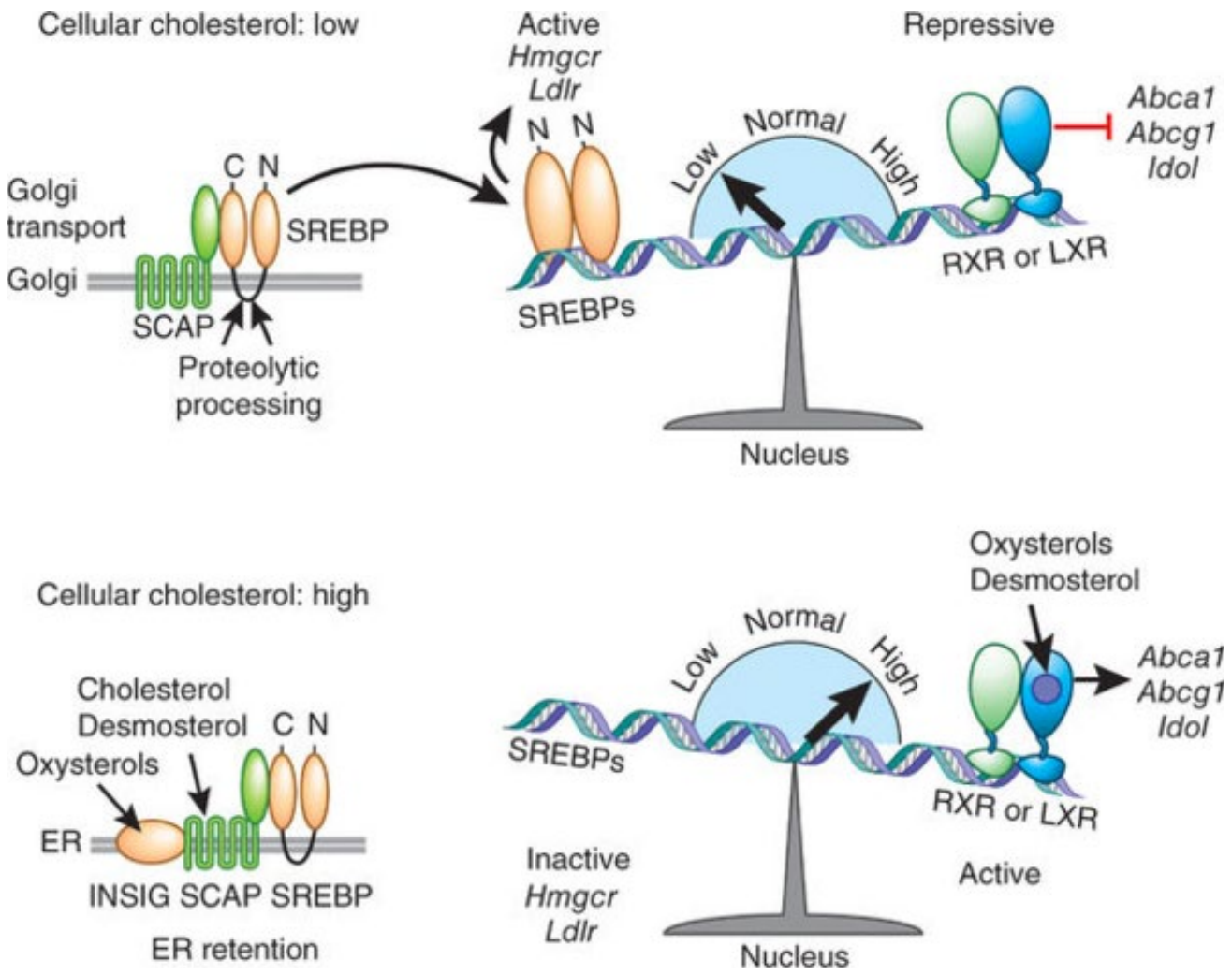

Spann and Glass. *Nature Immunology*. 2013; 14, 893–900.

KLF4 Transactivates Ch25h

A

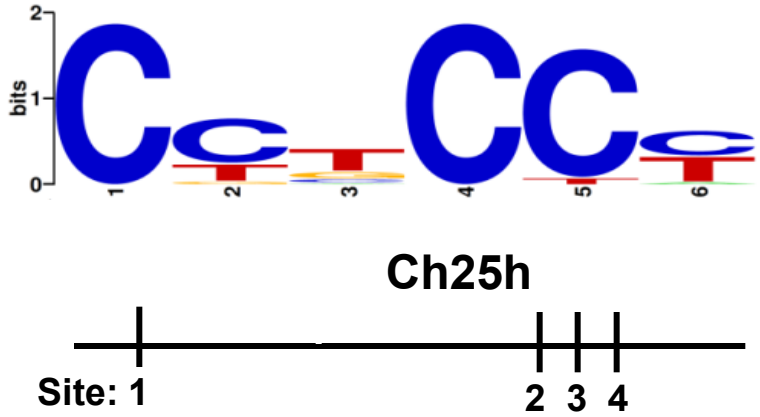

B

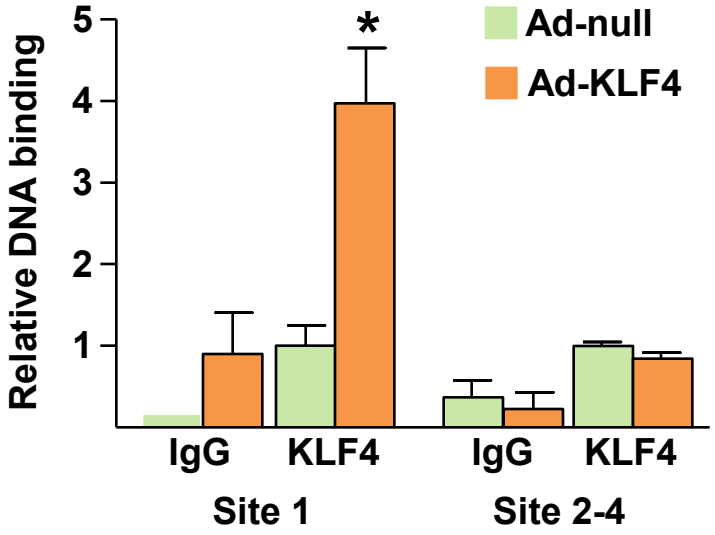

C

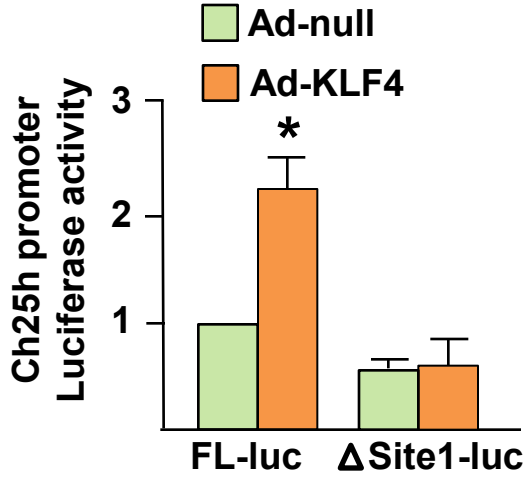

PS Regulation of Ch25h is Dependent on KLF4

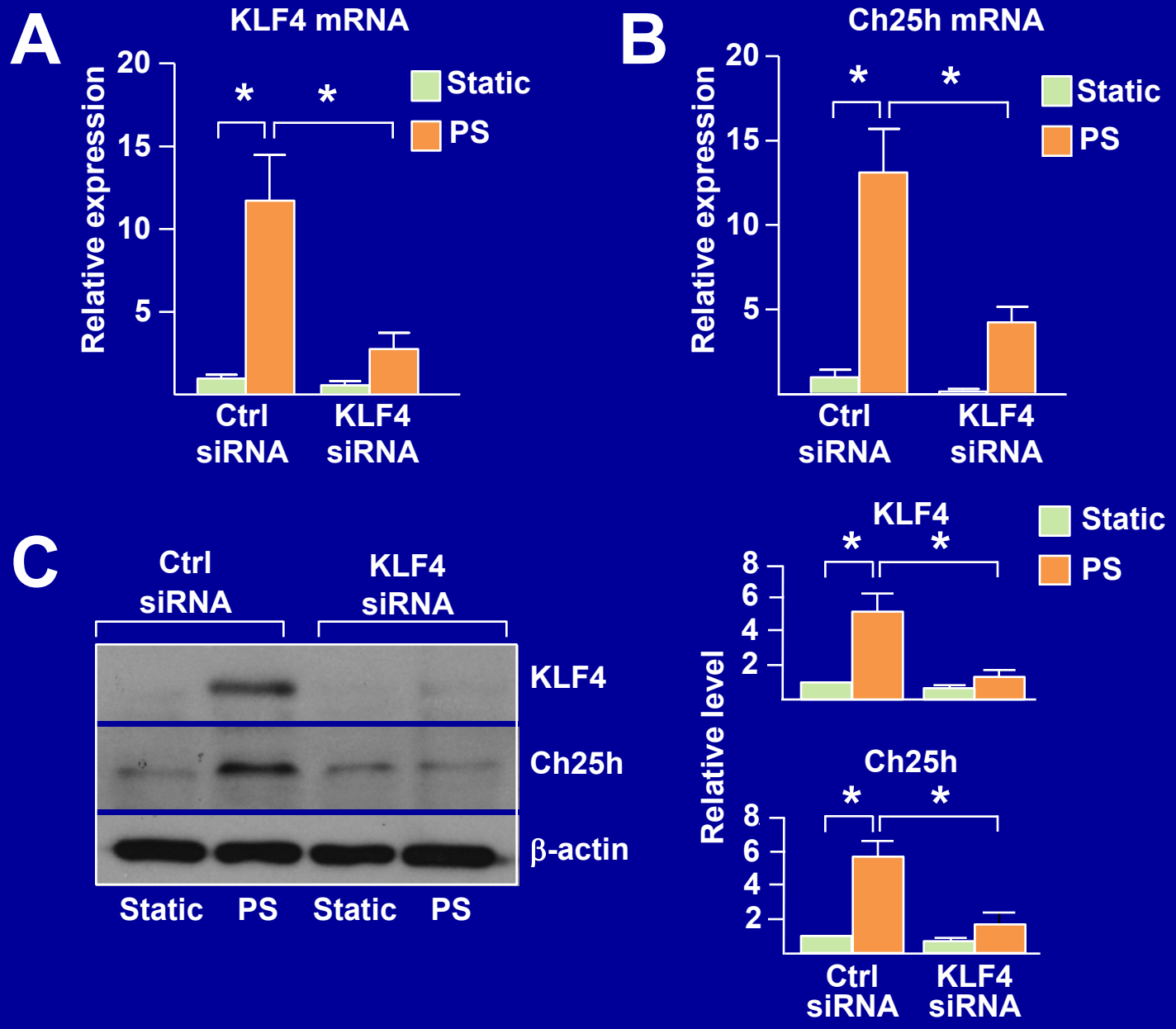

Epigenetic Regulation of the *Ch25h* promoter

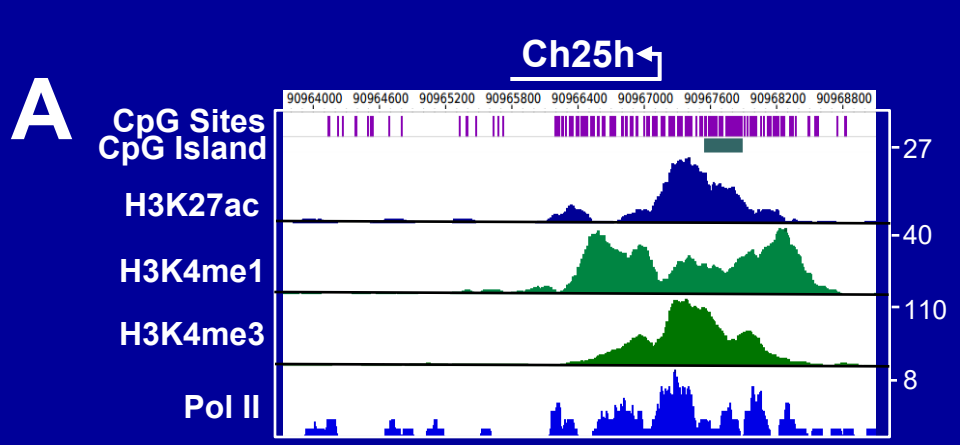

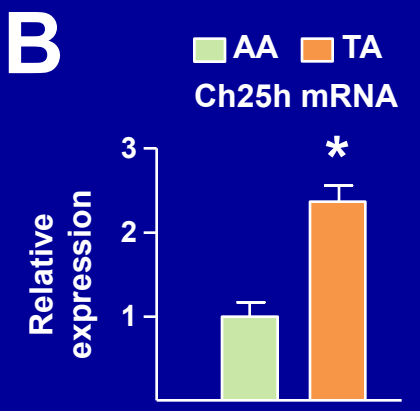

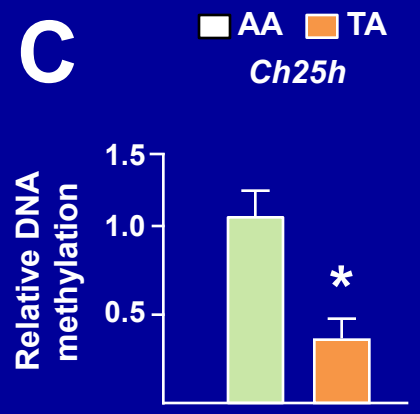

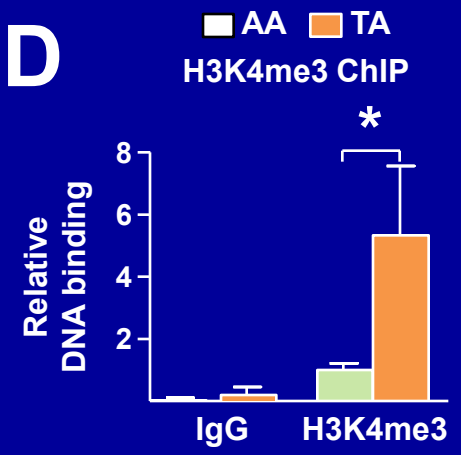

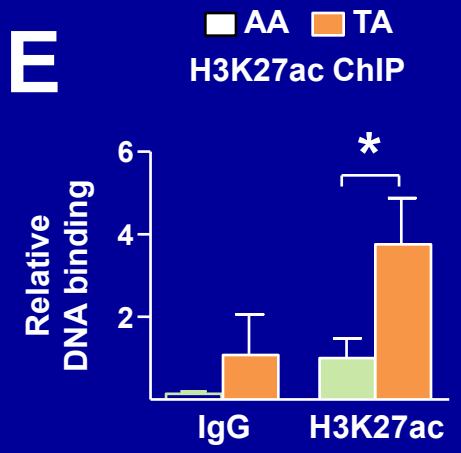

KLF4 transactivates LXRα

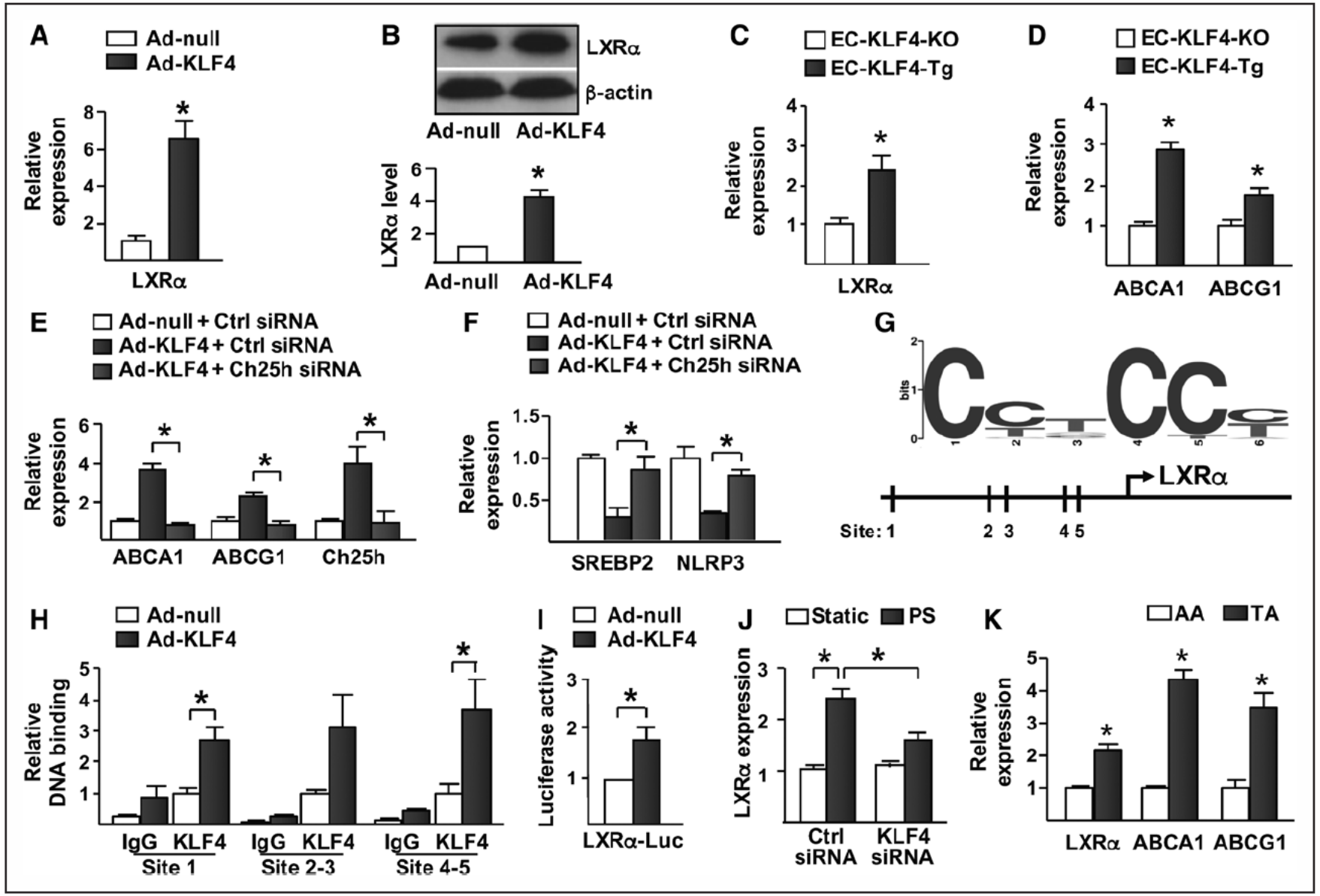

KLF4 Promotes LXRα Expression

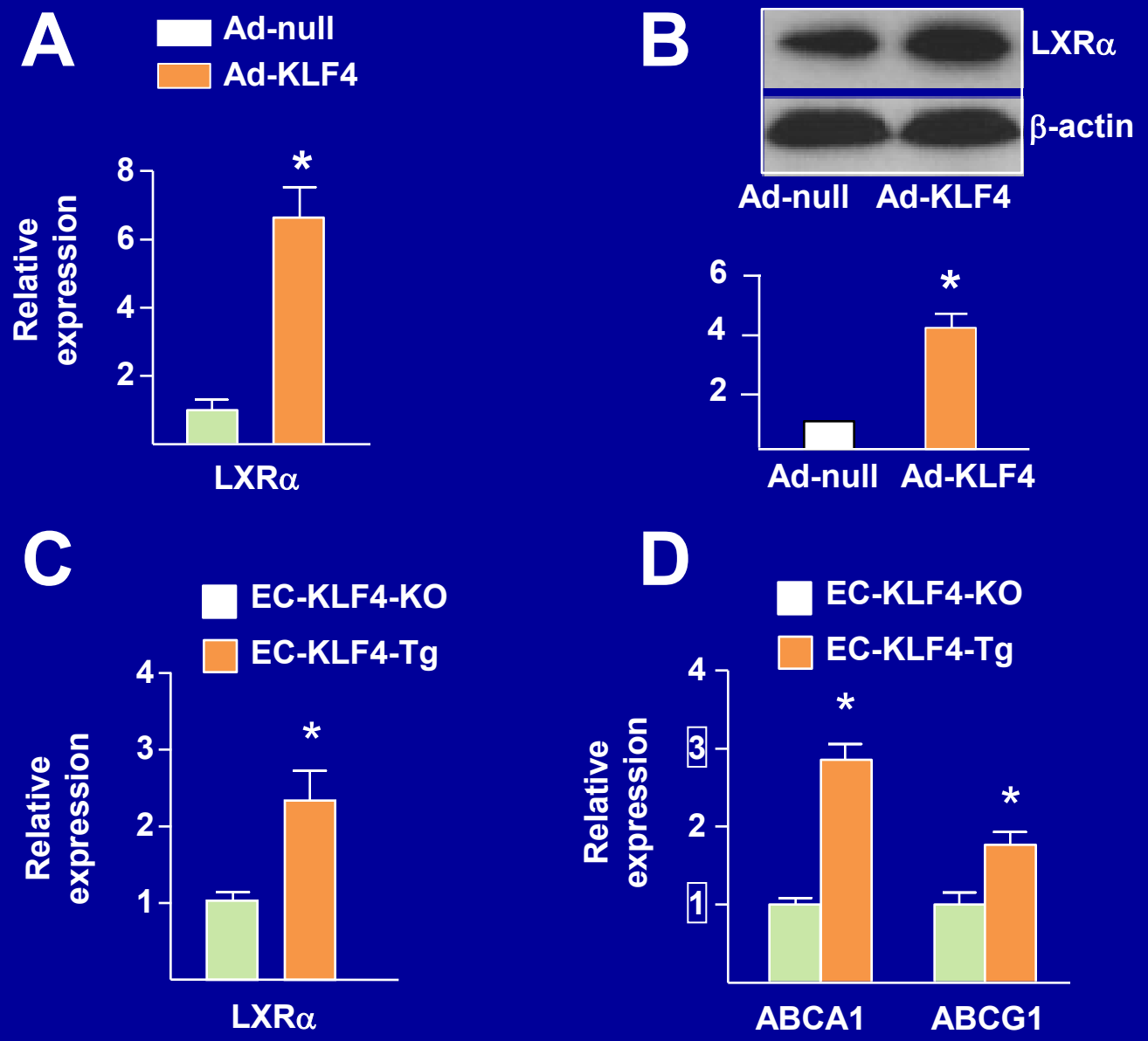

LXRα Expression is Dependent on Ch25h

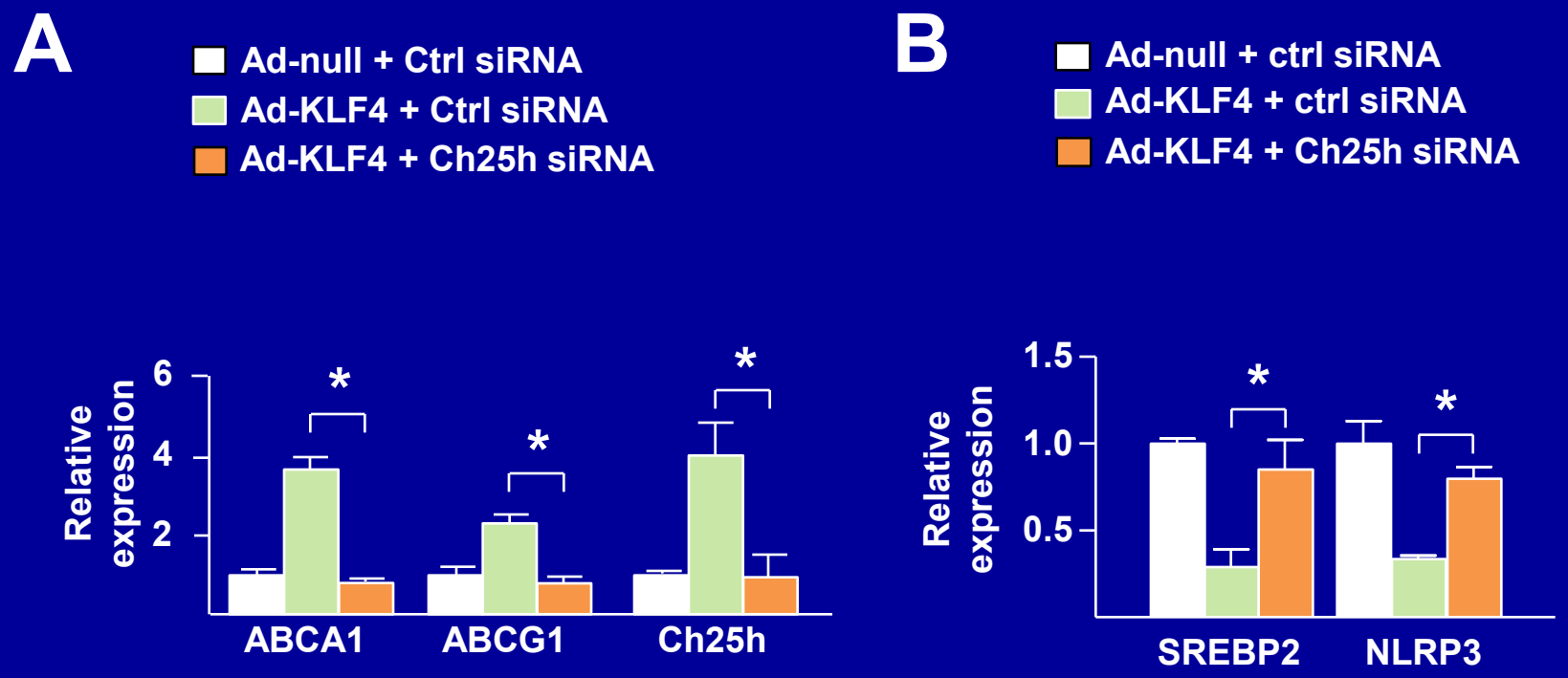

PS Regulation of LXRα in ECs Is KLF4-Dependent

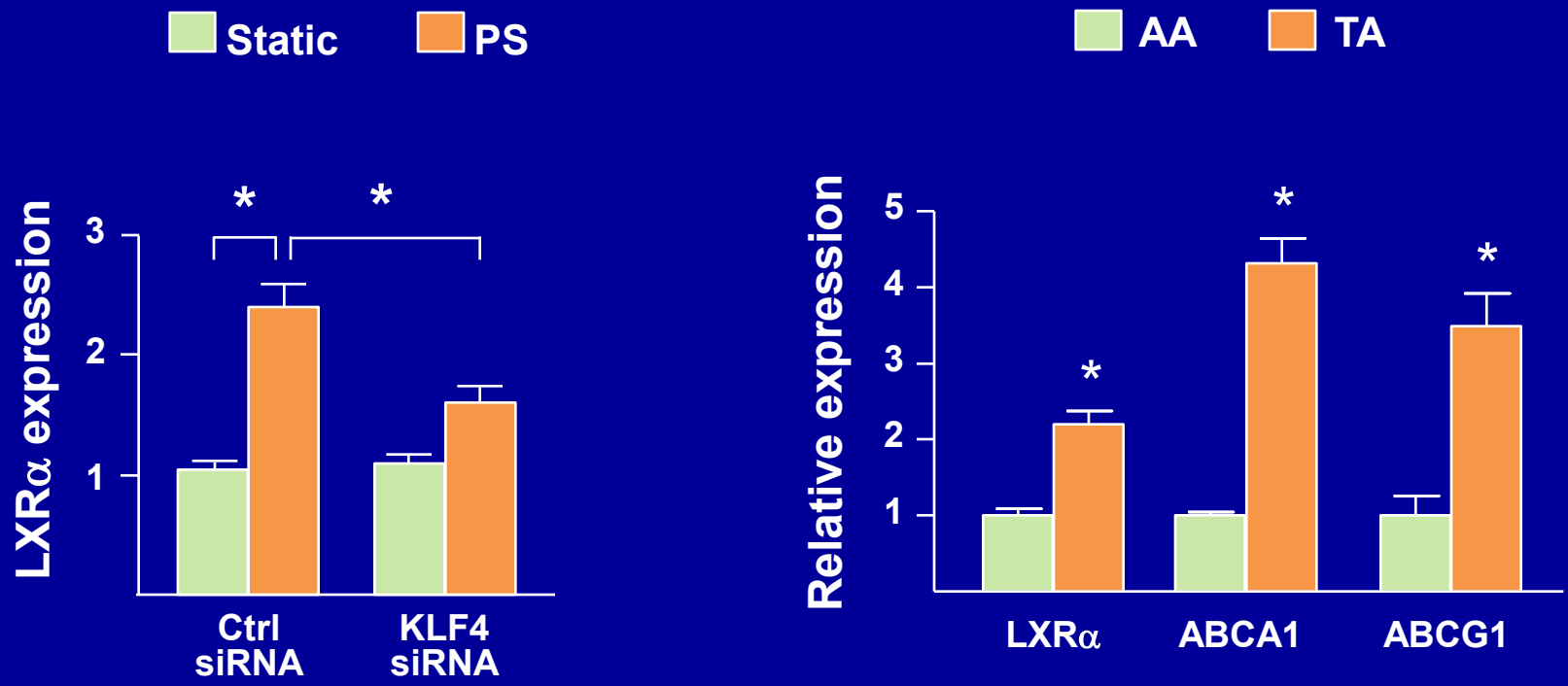

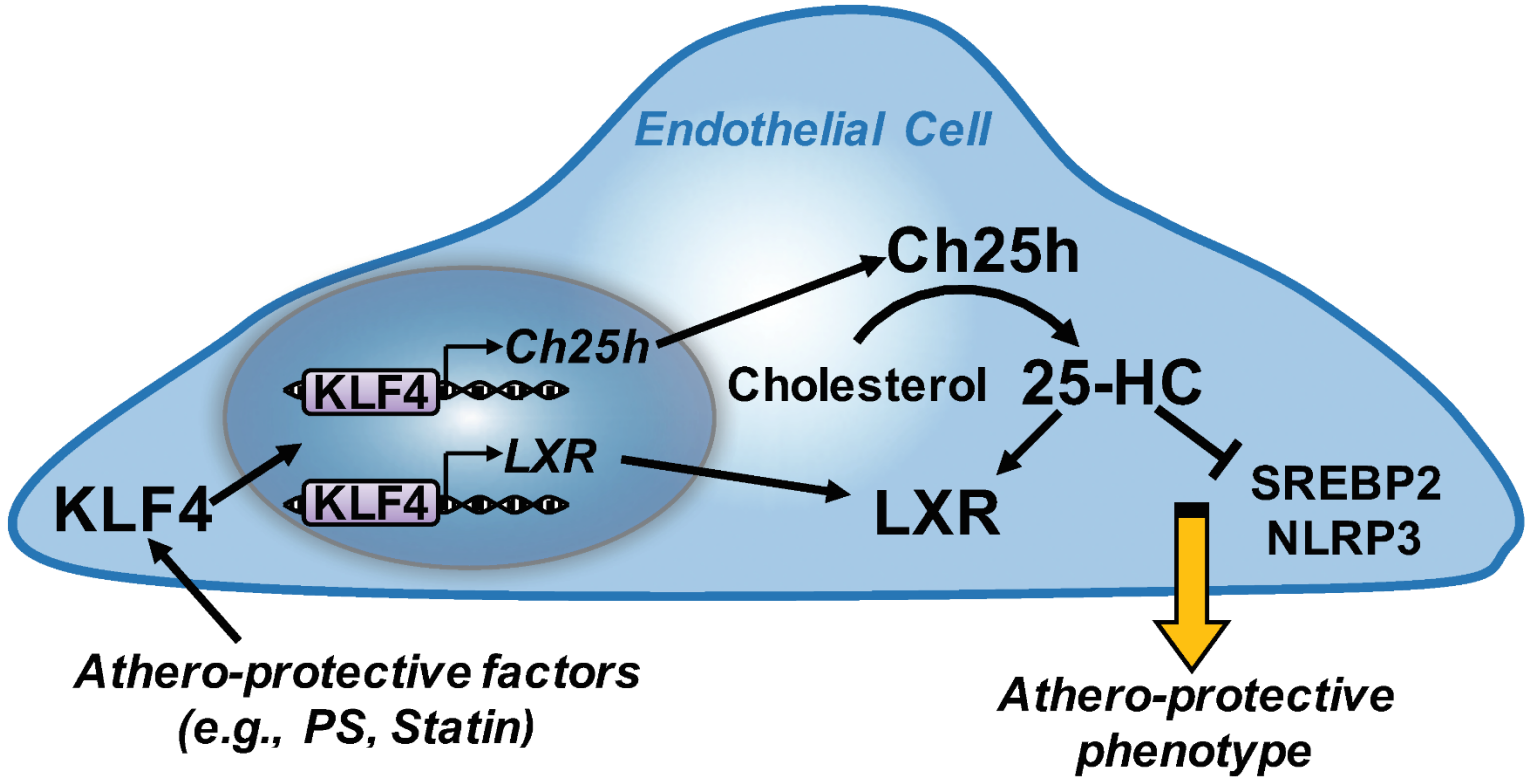

Inflammed Macrophage Cell

Defining Macrophage Inflammation
The LIPIDMAPS project

Gupta et al. J. Phys Chem B 2016
Gorden et al. J. Lipid Res. 2015
Farahangmehr et al., BMC Syst Biol. 2014
Masnadi-Shirazi et al., IEEE Trans Biomed Circuits Syst. 2014
Kihara et al., Biophys J. 2014
Shibata et al. J. Biol. Chem. 2013
Dinasarapu et al., Bioinformatics 2013
Maurya et al., J. Lipid Res. 2013
Spann et al., Cell 2012
Asad et al., IET Syst Biol. 2012
Subramaniam et al., Chem Rev. 2011
Dennis et al., J. Biol. Chem. 2010
Quenberger et al., J Lipid Res. 2010
Andreyev et al., J. Lipid Res. 2010
Andreyev et al., Mol. Cell Prot. 2010
Fahy et al., J. Lipid. Res. 2010
Gupta et al., BMC Systems Biol. 2011
Gupta et al., PLoS Comput. Biol. 2010
Gupta et al., Biophys J. 2009
Fahy et al., Nucleic Acid Res. 2009
Sud et al., Nucleic Acid Res. 2009
Maurya et al., Adv. Exp. Med. 2007
Fahy et al., Meth. Enzymology 2007
Pradervand et al., Genome Biol. 2006

Integration of lipidomics, transcriptomics, and biological networks in macrophage inflammation

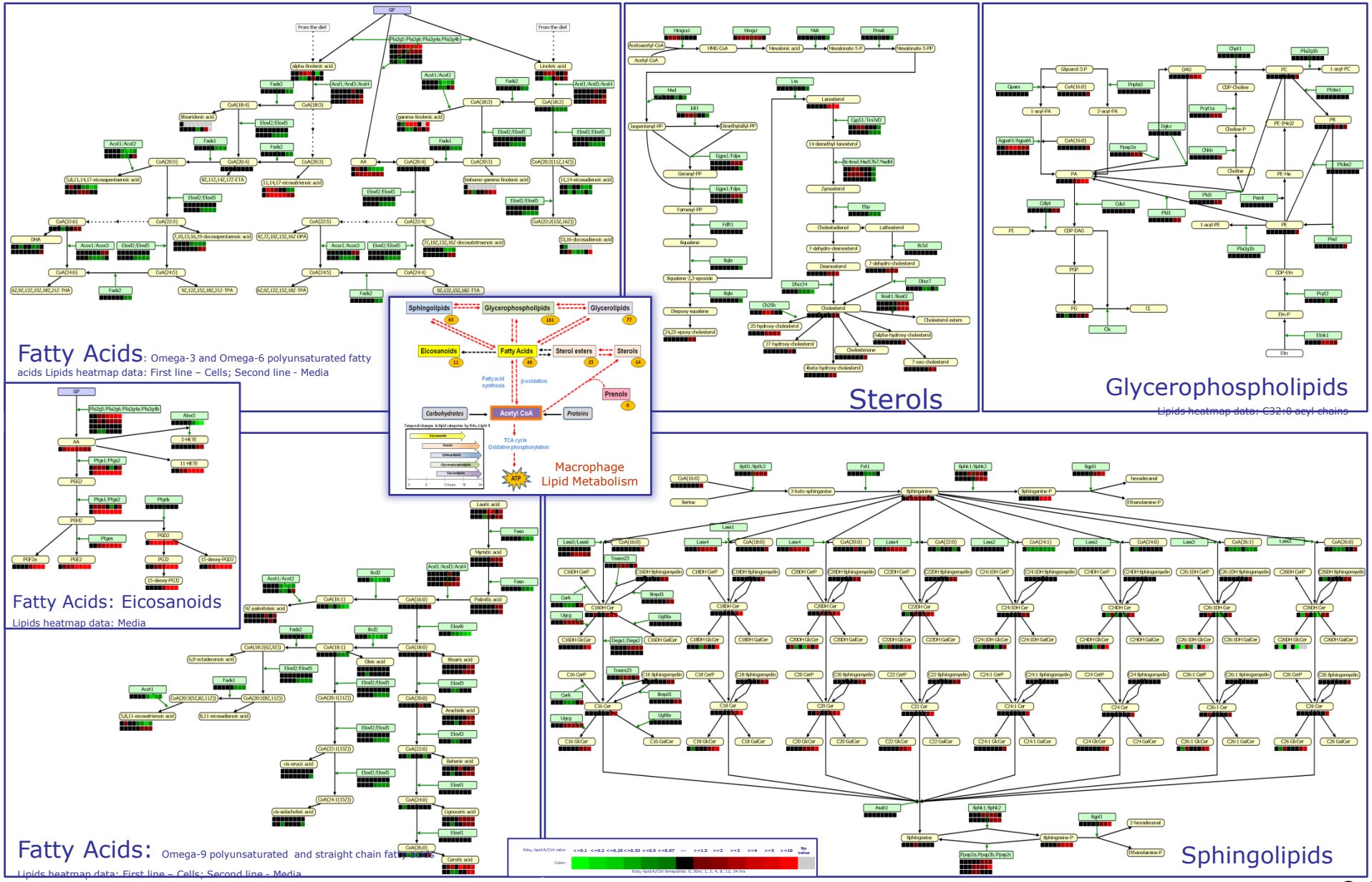

Dennis et al., J. Biol. Chem. 2010; Subramaniam, et al., 2011

Endothelial Cell - Inflammed Macrophage Cell Crosstalk

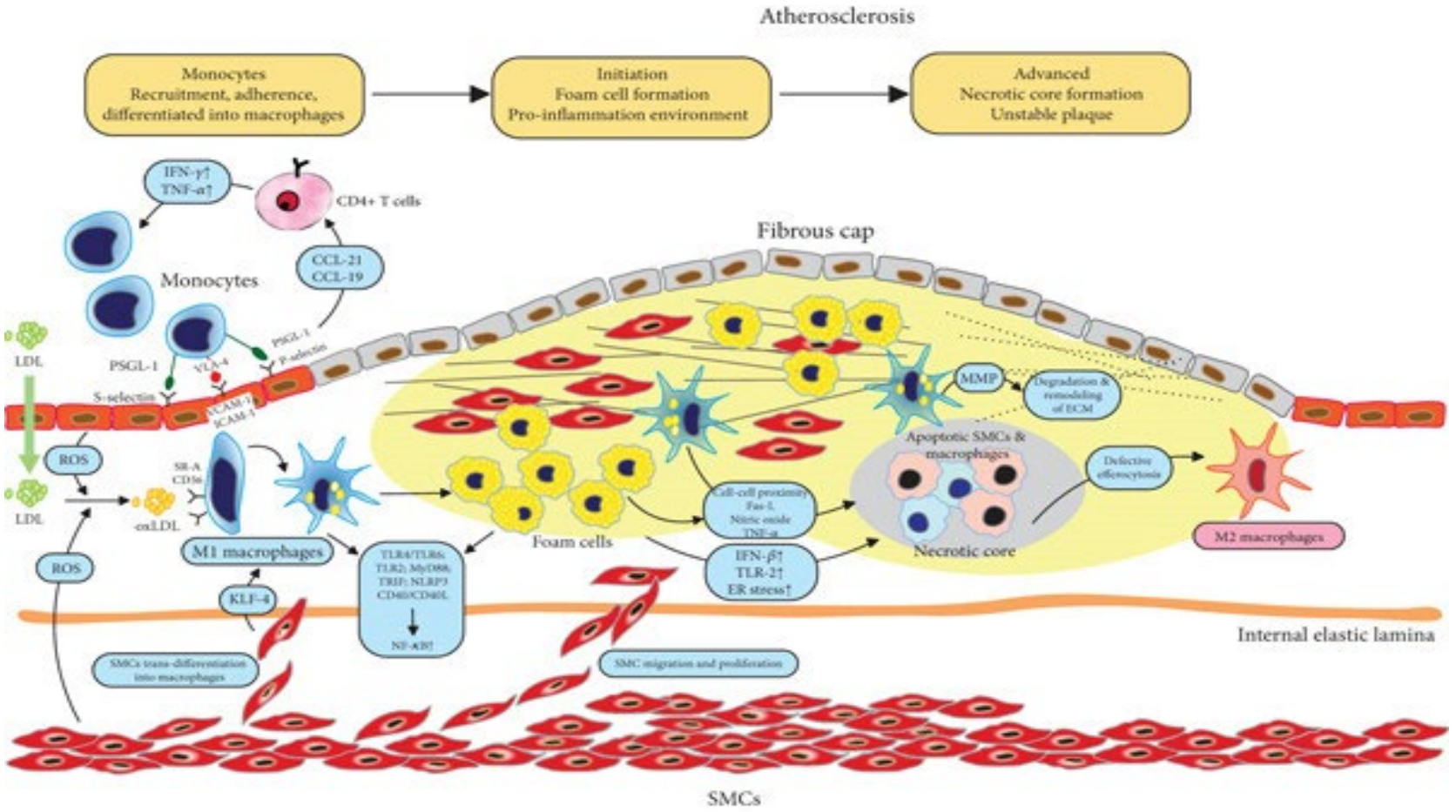

Journal of Immunology Research, Volume: 2019, Issue: 1, First published: 01 December 2019, DOI: (10.1155/2019/4354786)

Impaired Cholesterol Homeostasis in Ch25h$^{-/-}$ Macrophage

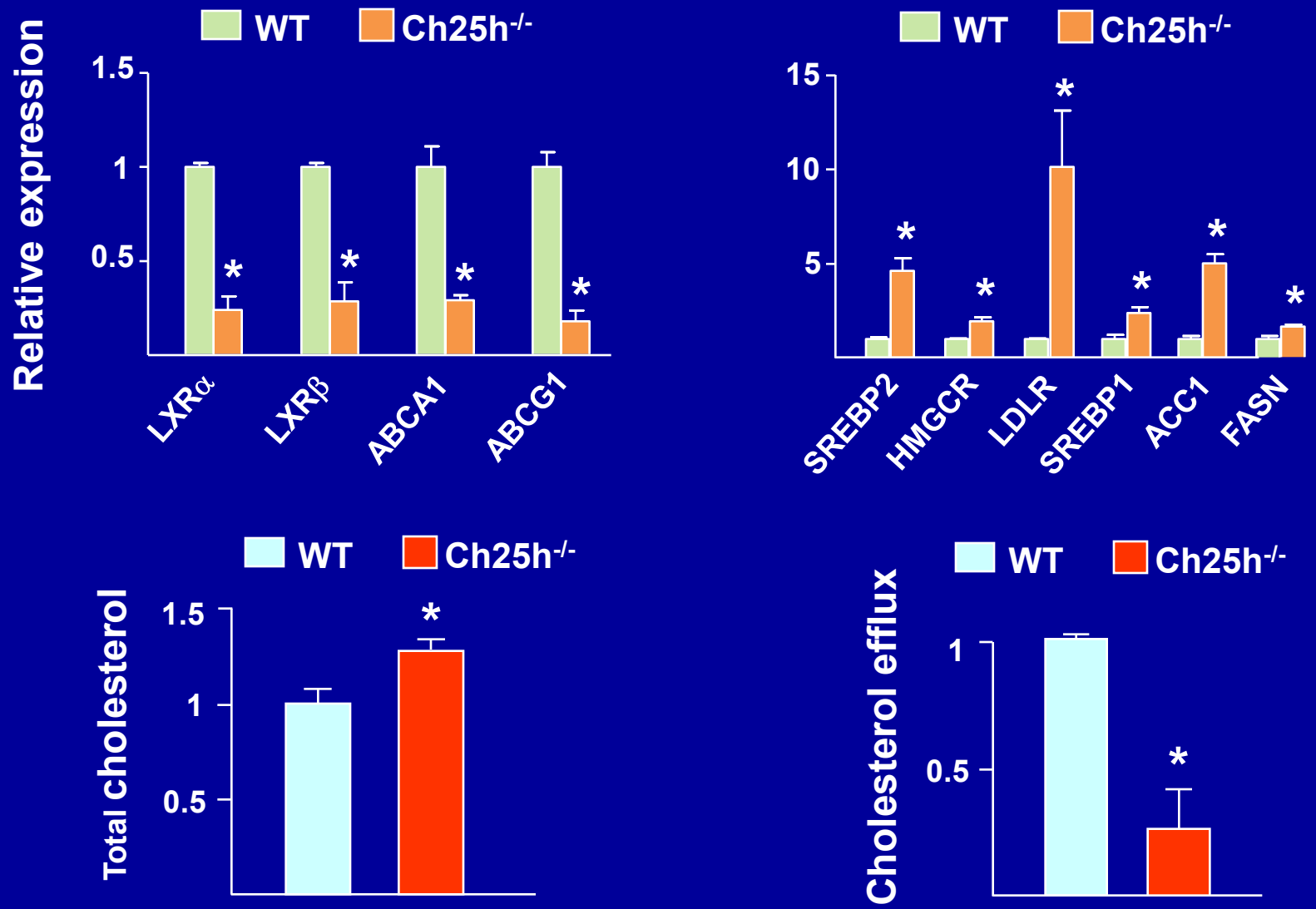

M2 Polarization in Ch25h$^{-/-}$ Macrophages

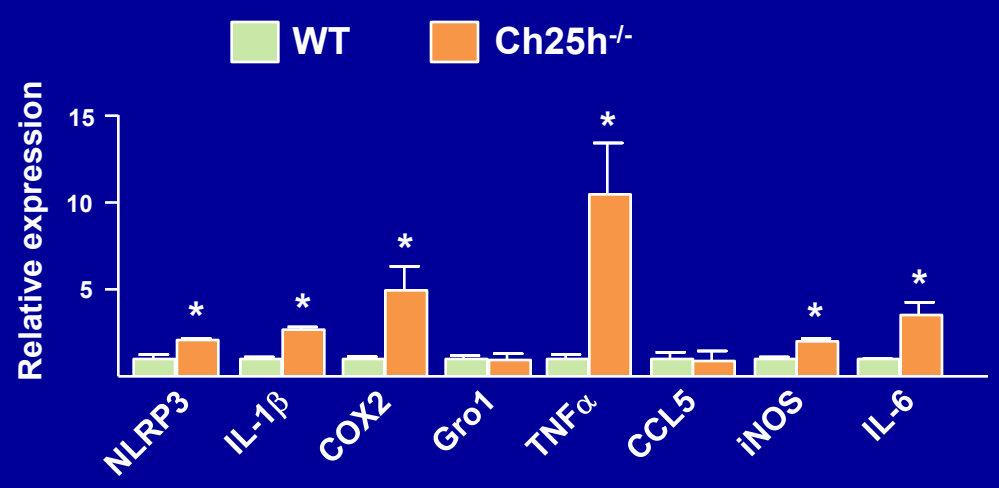

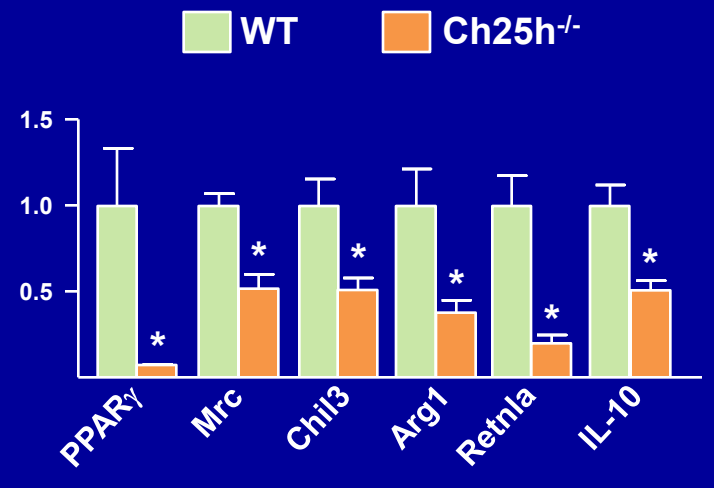

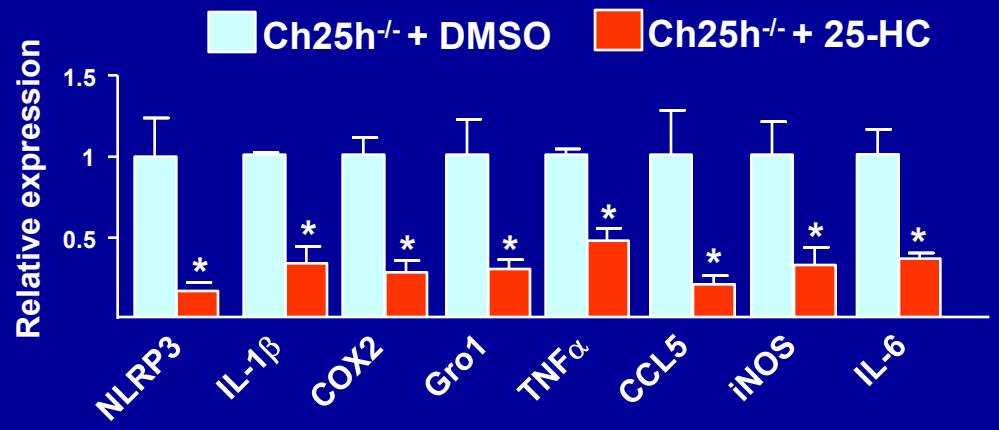

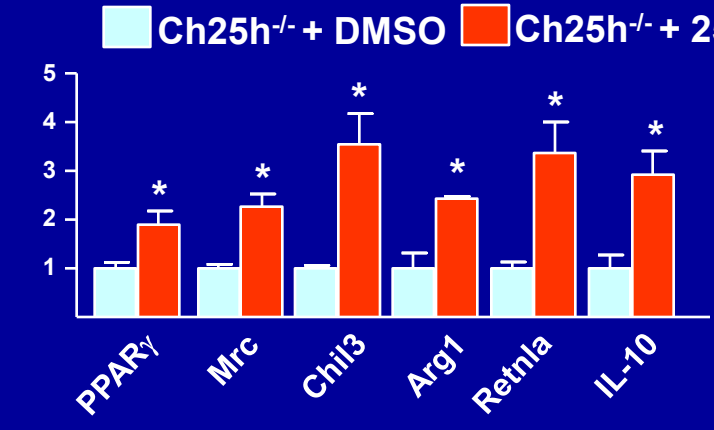

KLF4 regulation of Ch25h/LXR in Mϕ promotes M2 polarization

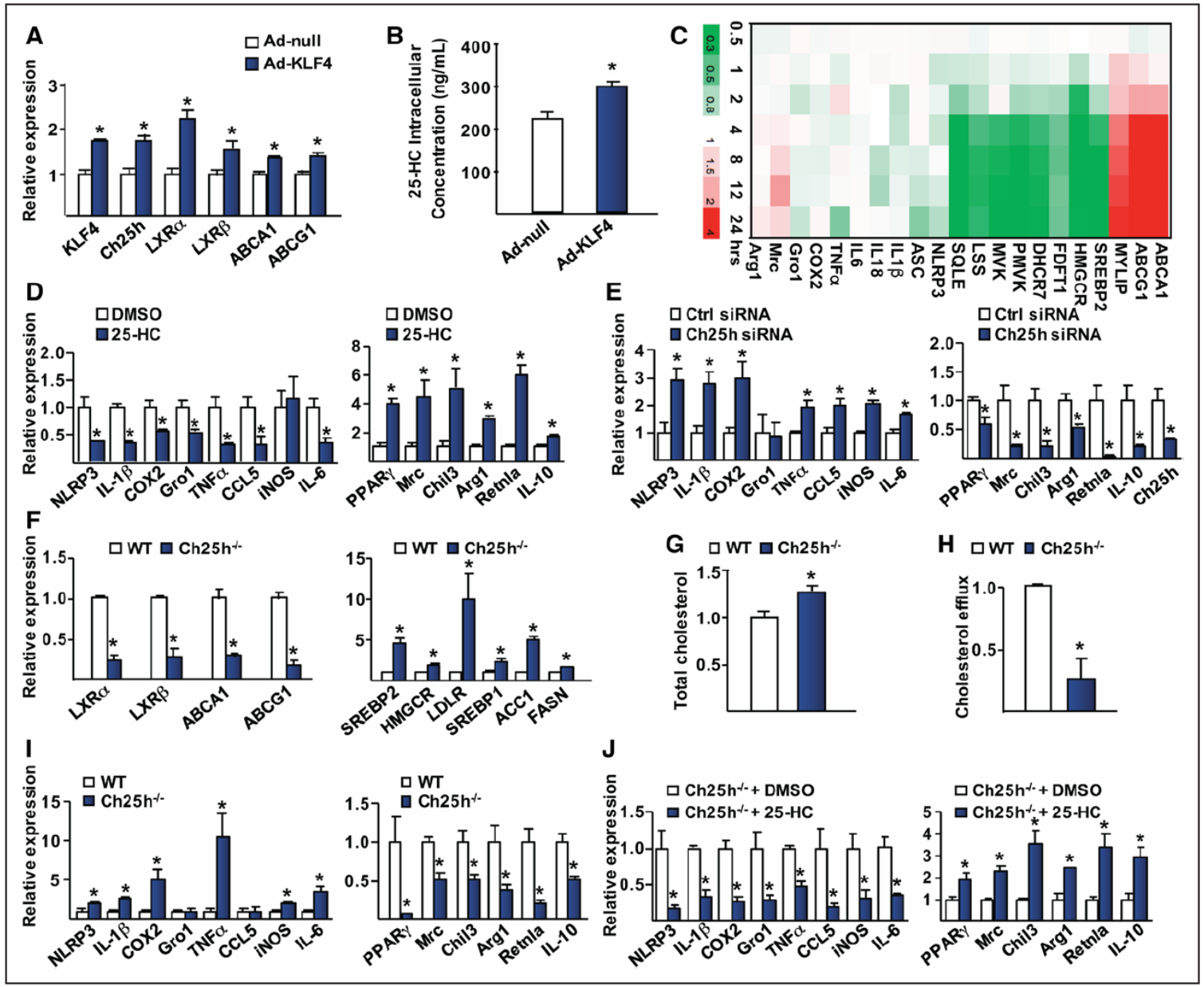

Ch25h ablation increases atherosclerosis susceptibility

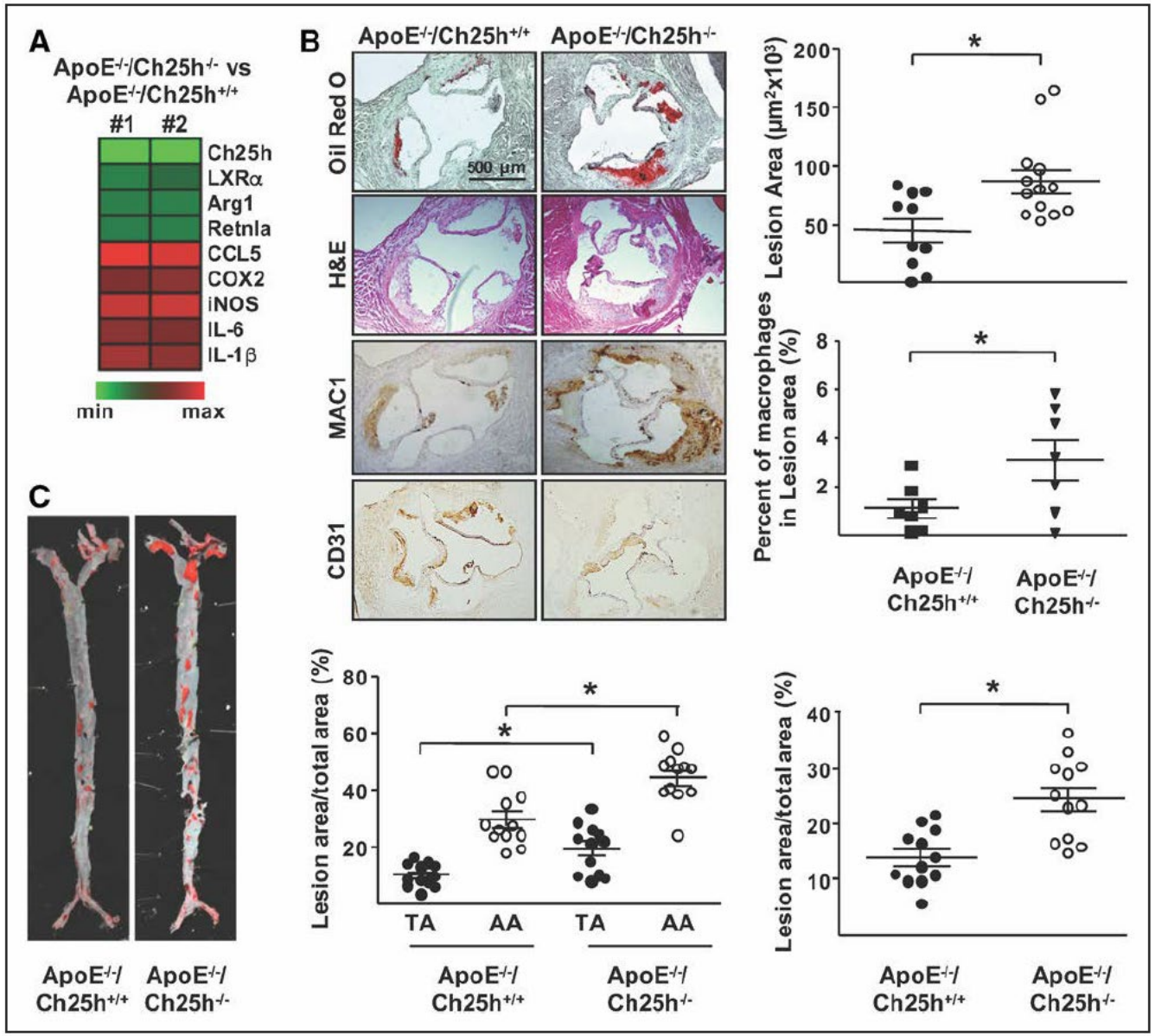

KLF4 mediates Ch25h and LXR in ECs and Mfs to promote atheroprotection